Geological Survey of Finland 2021

The Vaajasalmi flake graphite, Rautalampi, Central Finland

Janne Kuusela, Dandara Salvador, Jaakko Nurkkala, Esa Heilimo, Maarit Nousiainen, Timo Ahtola and Thair Al-Ani

GTK Open File Research Report 60/2021

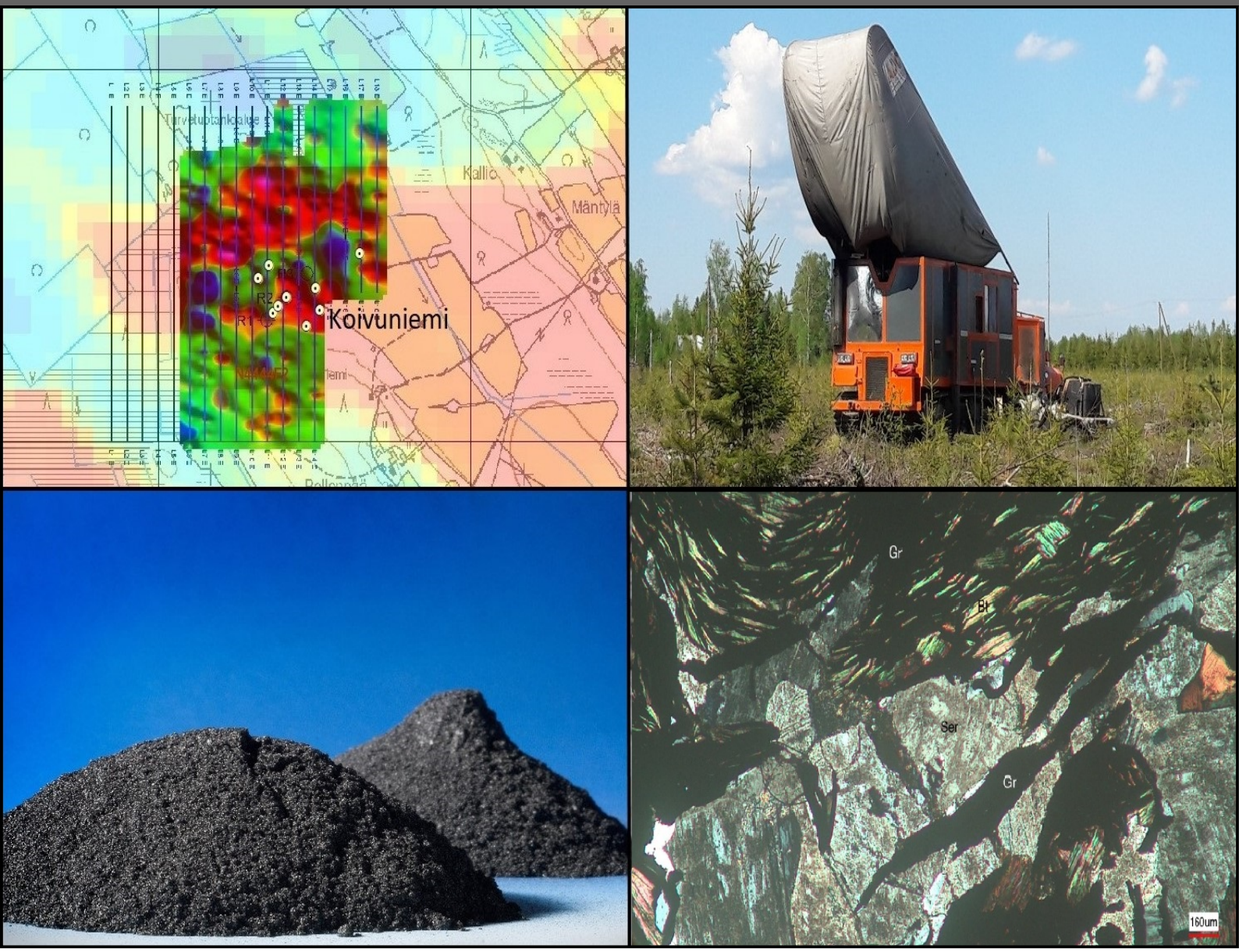

TURUN YLIOPISTO

GTK

GEOLOGICAL SURVEY OF FINLAND

Open File Research Report 60/2021

Janne Kuusela, Dandara Salvador, Jaakko Nurkkala, Esa Heilimo, Maarit Nousiainen,
Timo Ahtola and Thair Al-Ani

The Vaajasalmi flake graphite, Rautalampi, Central Finland

Unless otherwise indicated, the figures have been prepared by the authors of the report.

Front cover: The Vaajasalmi flake graphite: From discovery to beneficiation tests.
Photo by the authors.

Layout: Elvi Turtiainen Oy

Espoo 2021

Kuusela, J., Salvador, D., Nurkkala, J., Heilimo, E., Nousiainen, M., Ahtola, T. & Al-Ani, T. 2021. The Vaajasalmi flake graphite, Rautalampi, Central Finland. *Geological Survey of Finland, Open File Research Report 60/2021,* 34 pages, 25 figures, 11 tables and 4 appendices.

The Geological Survey of Finland discovered a new flake graphite mineralization in the Vaajasalmi area in the municipality of Rautalampi in Central Finland during the battery mineral project executed in 2016–2019. Airborne electromagnetic anomalies and earlier diamond drilling campaigns by Outokumpu Oy 3 km SW in the Pukkiharju area indicated strong graphite potential and resulted in the execution of a small drilling program in the Koivuniemi and Saareke targets. Preparatory work involving a ground geophysical slingram and magnetic measurements was carried out to direct the drillings. In a drilling campaign involving 13 diamond drill holes totaling 1263 m, the best intersection was 23.55 m @ 10.6% graphitic C (Cg) in the Koivuniemi target. The northernmost drill holes also reached a larger conductive anomalous area, suggesting that the anomaly is caused by the presence of flake graphite. The second target in Saareke contained significantly less graphite, with its best section being 6 m @ 3.6% Cg hosted by a more mafic volcanic rock type than in Koivuniemi. Important parameters controlling the economic value of graphite include the flake size, purity, and shape of the grains. The studied thin sections revealed that the graphite appears in various types, which may reflect the graphite being partially or fully remobilized due to partial melting. The longest axis of measured graphitic flakes ranged from 50–1000 µm. According to SEM studies, impurities inside the graphite grains typically contain the same material that surrounds them. Laboratory-scale beneficiation tests were conducted for a Koivuniemi sample in the GTK Mintec laboratory. The tests involved crushing, grinding, flotation, and purification by alkaline roasting and acid leaching. The result after the flotation scheme was a 91% graphitic concentrate with 82% recovery. After alkaline roasting and acid leaching, the graphitic concentrate reached a purity grade of over 99%.

Keywords: exploration, flake graphite, diamond drilling, beneficiation, Rautalampi, Central Finland

Janne Kuusela
Geological Survey of Finland
P.O. Box 96
FI-02151 Espoo, Finland

E-mail: janne.kuusela@gtk.fi

Kuusela, J., Salvador, D., Nurkkala, J., Heilimo, E., Nousiainen, M., Ahtola, T. & Al-Ani, T. 2021. The Vaajasalmi flake graphite, Rautalampi, Central Finland. Tiivistelmä: Vaajasalmen suomugrafiittiaihe, Rautalampi, Keski-Suomi. *Geologian tutkimuskeskus, Tutkimustyöraportti 60/2021,* 34 sivua, 25 kuvaa, 11 taulukkoa ja 4 liitettä.

Geologian tutkimuskeskus (GTK) löysi vuosina 2016–2019 toteutetun Akkumineraalit-projektin yhteydessä uuden suomugrafiittiesiintymän Rautalammin Vaajasalmesta. Outokumpu Oy:n 1970- ja 1980-lukujen vaihteessa suorittamat tutkimukset noin 3 km Vaajasalmesta lounaaseen sijaitsevalla Pukkiharju-nimisellä alueella sekä lentosähköiset anomaliat indikoivat suurta grafiittipotentiaalia myös Vaajasalmen alueelle. GTK teki alueella sähköisiä ja magneettisia geofysiikan maastomittauksia sekä timanttikairausta yhteensä 1 263 m Koivuniemen ja Saarekkeen kohteisiin. Parhaalla Koivuniemen grafiittilävistyksellä oli paksuutta 23,55 m, ja sen grafiittipitoisuus oli 10,6 %. Koivuniemen pohjoisin kairareikä ulottui laajempaan sähköiseen anomaliaan pohjoisessa ja antoi positiivisen viitteen suomugrafiitin esiintymisestä. Saarekkeen kairauksissa esiin tulleet grafiittipitoisuudet olivat selvästi pienempiä. Kohteen vallitsevana kivilajina oli mafisempi vulkaniitti. Analysoitujen grafiittipitoisten kerrosten yhteydessä ei noussut esiin merkittäviä metallipitoisuuksia. Suomugrafiitin taloudelliseen arvoon vaikuttavat sen raekoko, puhtaus ja muoto. Vaajasalmen grafiitin ohuthietutkimuksissa ilmeni, että grafiittisuomuja esiintyy erimuotoisina yksittäin ja kasaumina, mikä heijastanee grafiitin olevan osittain tai täysin uudelleen kiteytynyttä osittaisen sulamisen vuoksi. Grafiittisuomujen koko mitattuna c-akselin suunnassa on 50–1 000 µm. SEM-tutkimukset osoittivat, että grafiittisuomujen sisältä löytyneet sulkeumat sisältävät samaa ainesta, kuin on niiden ympärillä. Koivuniemen grafiittia koerikastettiin GTK:n Mintecin laboratoriossa Outokummussa. Rikastusprosessi sisälsi murskauksen, jauhatuksen, vaahdotuksen sekä rikasteen puhdistamisen pasutuksella ja happoliuotuksella. Vaahdotuksen jälkeen grafiittirikasteen puhtaus oli 91 % ja saanti 82 %. Pasutuksen ja liuotuksen jälkeen rikasteen puhtausaste ylitti 99 %.

Asiasanat: grafiittipotentiaali, suomugrafiitti, rikastuskoe, Rautalampi, Keski-Suomi

Janne Kuusela
Geologian tutkimuskeskus
PL 96
02151 Espoo

Sähköposti: janne.kuusela@gtk.fi

CONTENTS

1 INTRODUCTION 6
1.1 The Vaajasalmi investigation area 7
1.2 General geology 8

2 SURVEY DESCRIPTION 9

3 GEOPHYSICAL SURVEYS 10
3.1 Aerogeophysics 10
3.2 Vaajasalmi ground survey area 10
3.2.1 Magnetic survey results 11
3.2.2 Electromagnetic survey results 11
3.2.3 Example of combining magnetic and slingram data 13

4 DIAMOND DRILLING & BEDROCK GEOLOGY 15
4.1 Koivuniemi 15
4.2 Saareke 17

5 CHEMICAL ANALYSES 18
5.1 Element correlation plots 18

6 MINERALOGY 21
6.1 Sampling and petrographic analysis 21
6.2 Whole-rock methods 21
6.3 Scanning electron microscope methods 21
6.4 Description of results 21
6.5 Detailed petrographic observations 23
6.6 SEM-EDS and whole-rock analyses 27
6.7 Summary of mineralogy 27

7 BENEFICIATION 28
7.1 Sample preparation 28
7.2 Analytical Methods 29
7.3 Methods for testing 29
7.4 Feed Samples 29
7.5 Flotation testing 29
7.6 Purification tests with alkaline roasting and acid leaching 32

8 CONCLUSIONS AND RECOMMENDATIONS 33

AKNOWLEDGEMENTS 34

REFERENCES 34

APPENDICES 35
Appendix 1. Laboratory analysis information
Appendix 2. Drillholes and drillhole profiles
Appendix 3. SEM-EDS – analysis data. Numbering after sample-id indicate spot analysis number
Appendix 4. Detailed list of petrographical observations and carbon contents of whole rock-analysis

1 INTRODUCTION

The Rautalampi–Suonenjoki area has been of mineral potential interest regarding Ni, Cu, and Zn, and has therefore undergone several exploration programs by Outokumpu since the 1950s. The area is mainly composed of volcano-sedimentary associations that can be observed as an accumulation of geophysical anomalies via which the geology of the poorly outcropped terrain has been partly interpreted (Koistinen 1982). During 1977–1982, an exploration program with 17 diamond drill holes was carried out in Pukkiharju and the Käpysuo area with the aim of locating the source of several Zn-bearing boulders found in the area. The drilling program resulted in multiple penetrations of graphite-rich layers, but did not at the time lead to further investigations.

With the rapidly increasing need for graphite as a material for the refractories industry and an anode material in Li-ion batteries, the Geological Survey of Finland started a battery mineral project in 2016. The Outkokumpu drill cores were reviewed and assessed to contain substantial amounts of flaky graphite (Al-Ani et al. 2018). The conductive anomalies revealed by airborne geophysical sounding continue to the east towards the Vaajasalmi area, nearly as wide as in Käpysuo. A typical feature in

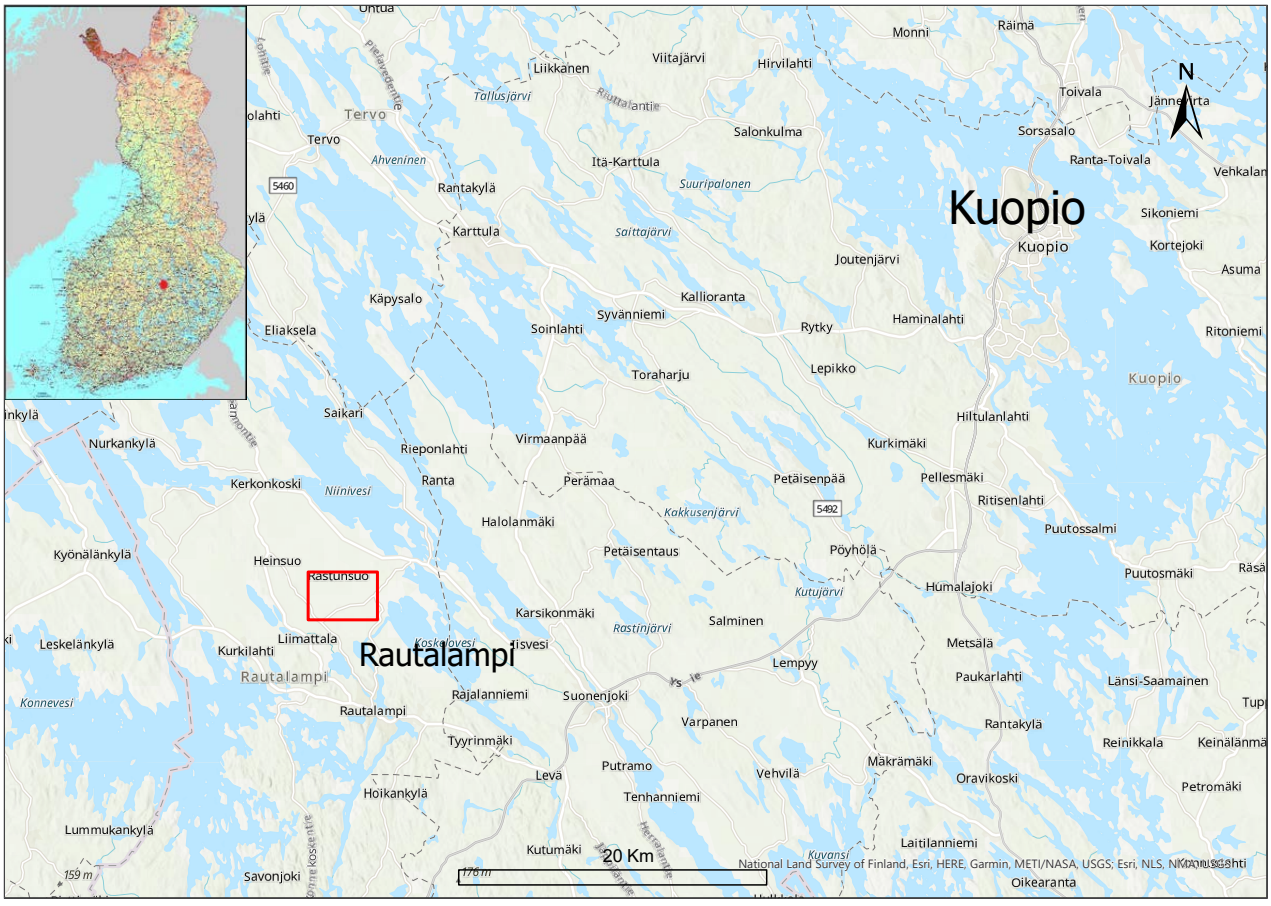

Fig. 1. Location of the Vaajasalmi investigation area, denoted by a red rectangle (Finland basemap, Bedrock of Finland – DigiKP).

the study area is abundant fault zones cutting the bedrock into brittle blocks (Pääjärvi 2000). Based on these anomalies and indicative structural markers, GTK decided to investigate the possible extension of the graphite-bearing layers towards the east in targets at Koivuniemi and Saareke, which are located 3 km NE of the Käpysuo area.

Another exploration program similiar to the one described in this report was also performed in the Käpysuo target (Pukkiharju) during 2017 and 2018 (Al-Ani et al. 2020). The exploration program in Vaajasalmi was comprised of ground geophysics, diamond drilling and a mineralogical quality assessment of the flake graphite, which also included laboratory-scale beneficiation testing by GTK Mintec Outokumpu. This report concentrates on the investigations conducted in the Vaajasalmi targets.

1.1 The Vaajasalmi investigation area

During 2017 and 2018, mineral potential studies were conducted in two targets, Koivuniemi and Saareke, in Vaajasalmi. Vaajasalmi is located in the municipality of Rautalampi, which is about 60 km SW of the city of Kuopio. The closest railroad connection is 14 km to the east in the city of Suonenjoki. The map sheet is N444 ETRS-TM35FIN. The results in Koivuniemi indicated a high potential, and GTK therefore decided to apply for an exploration permit covering an area of 50 ha, which is still (15.10.2021) under processing. All the investigations so far have been conducted with the consent of the landowners.

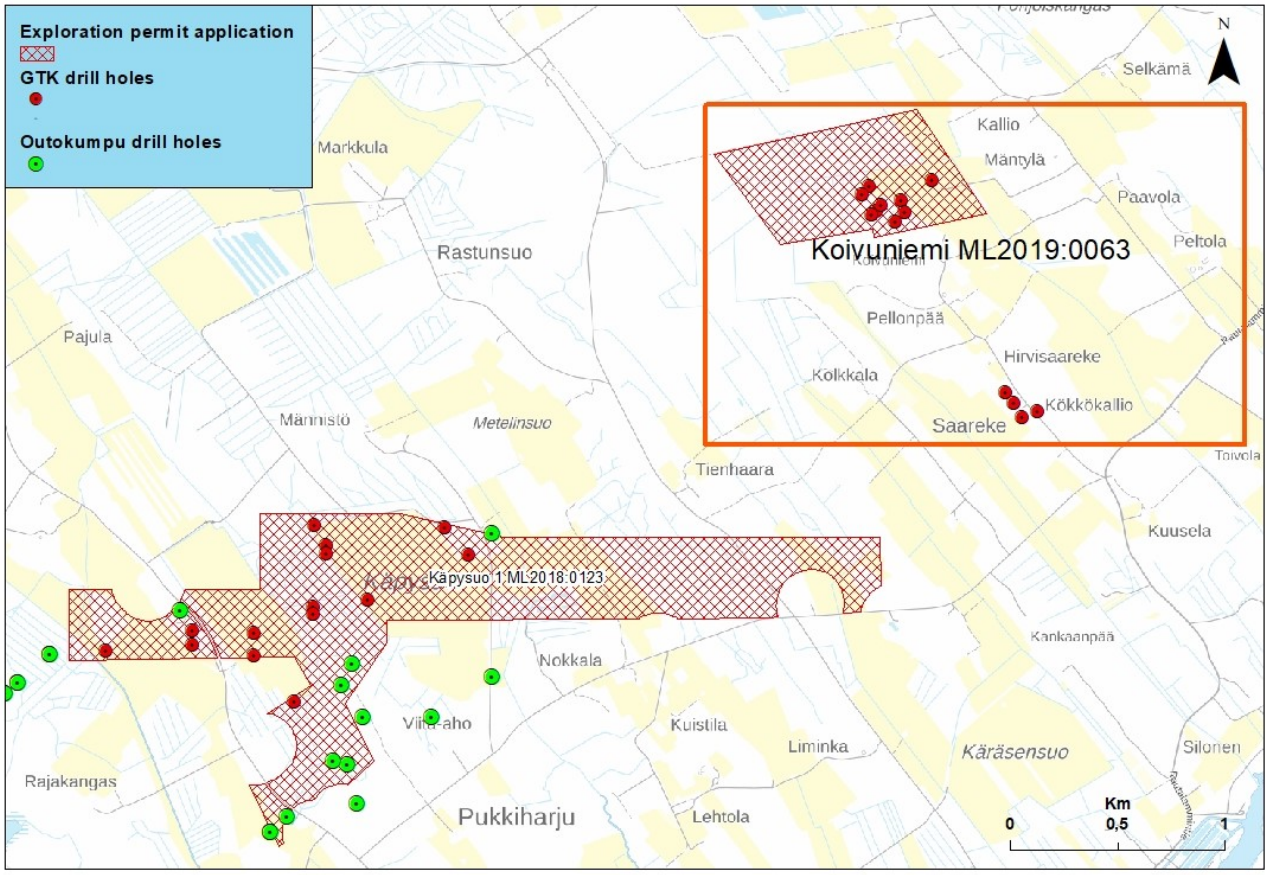

Fig. 2. The Rautalampi flake graphite targets for which exploration permits have been applied (Vaajasalmi area in the red rectangle). The drilling programs performed by GTK were executed during 2017 and 2018 (Mining register Finland and basemaps: © National Land Survey of Finland).

1.2 General geology

The Vaajasalmi area is a part of the Savo schist belt and is bordered by granitic blocks in the NE and SW. The geology of the area of interest is mainly composed of felsic gneisses with intermediate and mafic metavolcanic horizons that tend to have thick graphite rich layers. The presence of graphite horizons can, due to their conductive nature, be observed in airborne geophysical maps, as seen in Figure 5. According to Hölttä & Heilimo (2017), the metamorphic grade is for the most part granulite facies, which favors the formation of graphite with large flake sizes of >150 µm (Fig. 4). These rocks are, according to Lahtinen (1984), aged from 1.91–1.93 Ma. The Vaajasalmi area is cut in the east by a major NW–SE-trending fault, the so-called Iisvesi fault (Koistinen 1982). Another major fault located between the Vaajasalmi and Käpysuo areas has by transpressional movement separated the Vaajasalmi area from the Käpysuo area. The sinistral strike slip of the Vaajasalmi area northwards is most clearly visible in the geophysical conductive maps (Fig. 5).

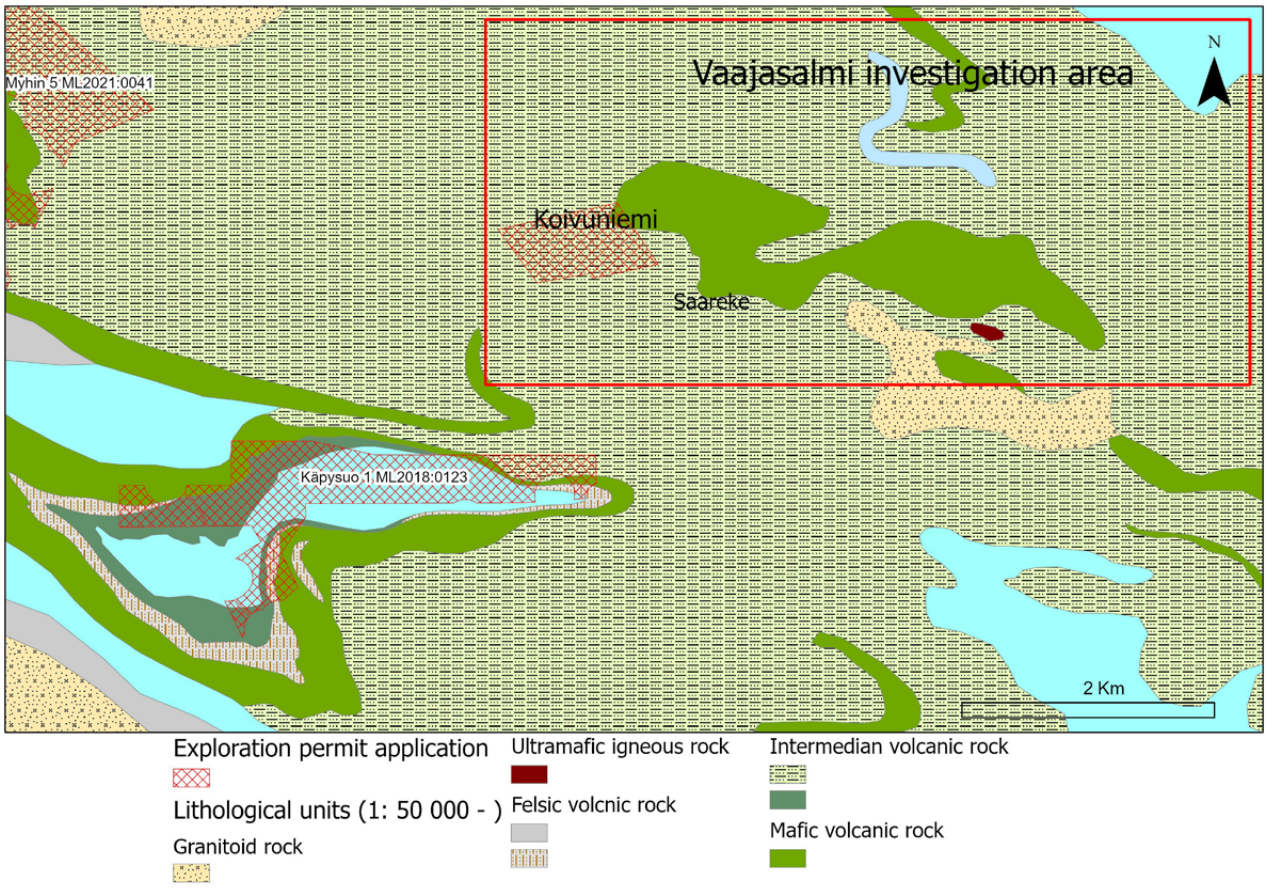

Fig. 3. Geological map of the Vaajasalmi investigation area (Source: bedrock map 1:50 000, Bedrock of Finland – DigiKP).

Fig. 4. Metamorphic facies map according to Hölttä & Heilimo (2017) with the investigation area indicated by a red star (Source: Metamorphic map 1:10 000 000, Bedrock of Finland – DigiKP).

2 SURVEY DESCRIPTION

The first drilling campaign was planned based on the structural interpretation of airborne electromagnetic maps (3 kHz) of Koivuniemi. Graphite-rich rocks are fragile and poorly able to withstand weathering, which makes outcropping graphitic rocks a rarity. This is also the case in the Rautalampi area, especially within the locations recognized to have the highest conductive anomalies. A ground geophysical program was executed in both Koivuniemi (75 ha) and Saareke (25 ha) targets (Figs. 6–9).

The results were not available for the first drilling campaign in Koivuniemi. The second drilling campaign was conducted in 2018 in the Saareke target. In the two drilling campaigns, 13 drillholes were drilled, totaling 1263 m. The drill cores were logged in the national drill-core archive in Loppi. As a result of the drill-core logging, 156 samples were sent for analysis. For mineralogical analyses, including SEM, 14 thin sections were prepared. The mineralogical studies were conducted at the University of Turku as a part of a Master's thesis project (Nurkkala 2021). To perform laboratory-scale first-stage beneficiation testing, a drill-core sample weighing 16 kg was sent to GTK Mintec in Outokumpu.

3 GEOPHYSICAL SURVEYS

3.1 Aerogeophysics

The whole Finland has been covered by aerogeophysical surveys conducted by GTK (Hautaniemi et al. 2005) using magnetic, radiometric and frequency domain electromagnetic (EM) methods. The Vaajasalmi survey site in Rautalampi belongs to the Karttula flight area, which was flown in 1986. The mean survey altitude in the Karttula area was 38 meters and the flight direction north–south, with a line separation of 200 m. In 1986, one measuring frequency used in the electromagnetic survey, which was 3113 Hz. The magnetic recording were made using 3 proton magnetometers, located in both wingtips and in the tail boom.

The EM data from the airborne survey are presented in Figure 5. Large EM anomalies can be seen in the Käpysuo and Vaajasalmi areas.

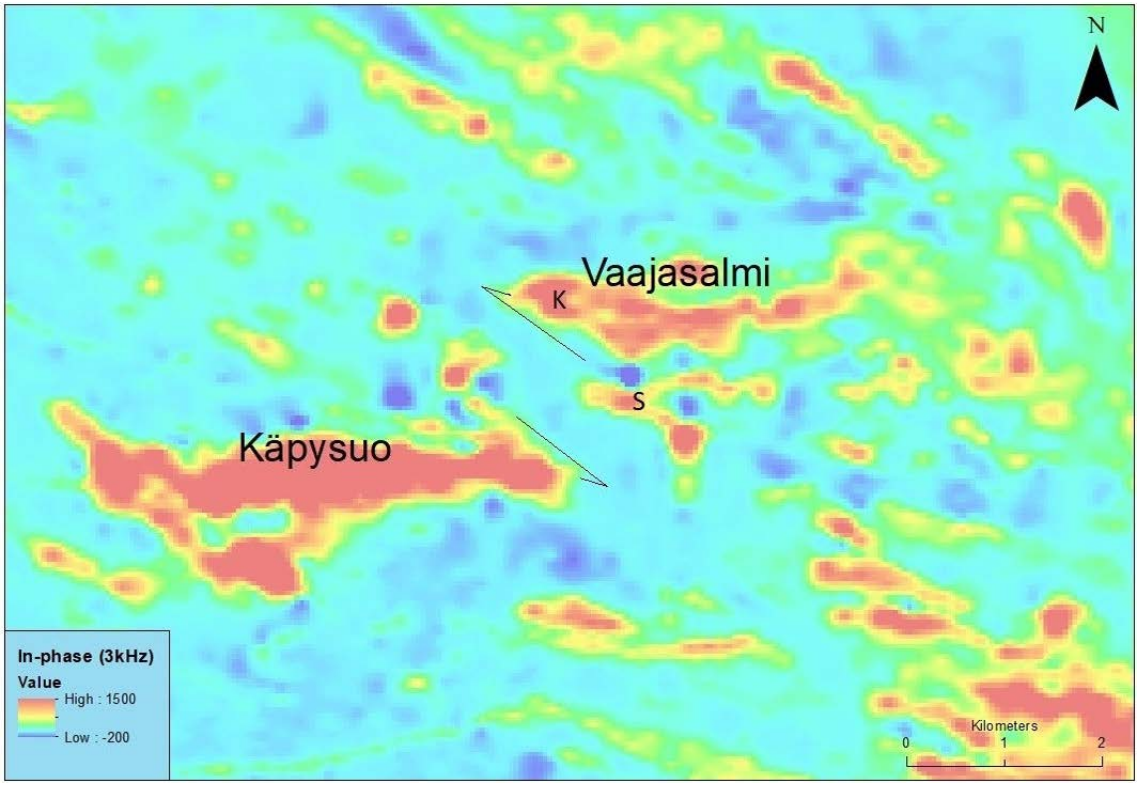

Fig. 5. Airborne geophysical in-phase (3 kHz) of the Vaajasalmi and Käpysuo areas with the Vaajasalmi targets K (Koivuniemi) and S (Saareke) indicated. Also highlighted is the interpretation of the transpressional sinistral strike slip faulting with resulting shear folding. Geophysical map from aerogeophysical data, Bedrock of Finland – DigiKP.

3.2 Vaajasalmi ground survey area

The area of geophysical surveys in Vaajasalmi was selected based on the aerogeophysical data and geological information. Powerlines can disturb the measurement, so they were avoided. Houses were also avoided. The line direction was north–south and was chosen to cross the geophysical features seen in the airborne data. The surveys covered two subareas, Koivuniemi in the north and Saareke in the south, with a line separation of 50 meters.

Regarding GTK's geological map, the southern survey area, Saareke, is located on intermediate tuff. In the northern survey area, Koivuniemi, there is also mafic vulcanite in addition to intermediate tuff. The geological map is simple, so it does not explain the features seen in the aeromagnetics.

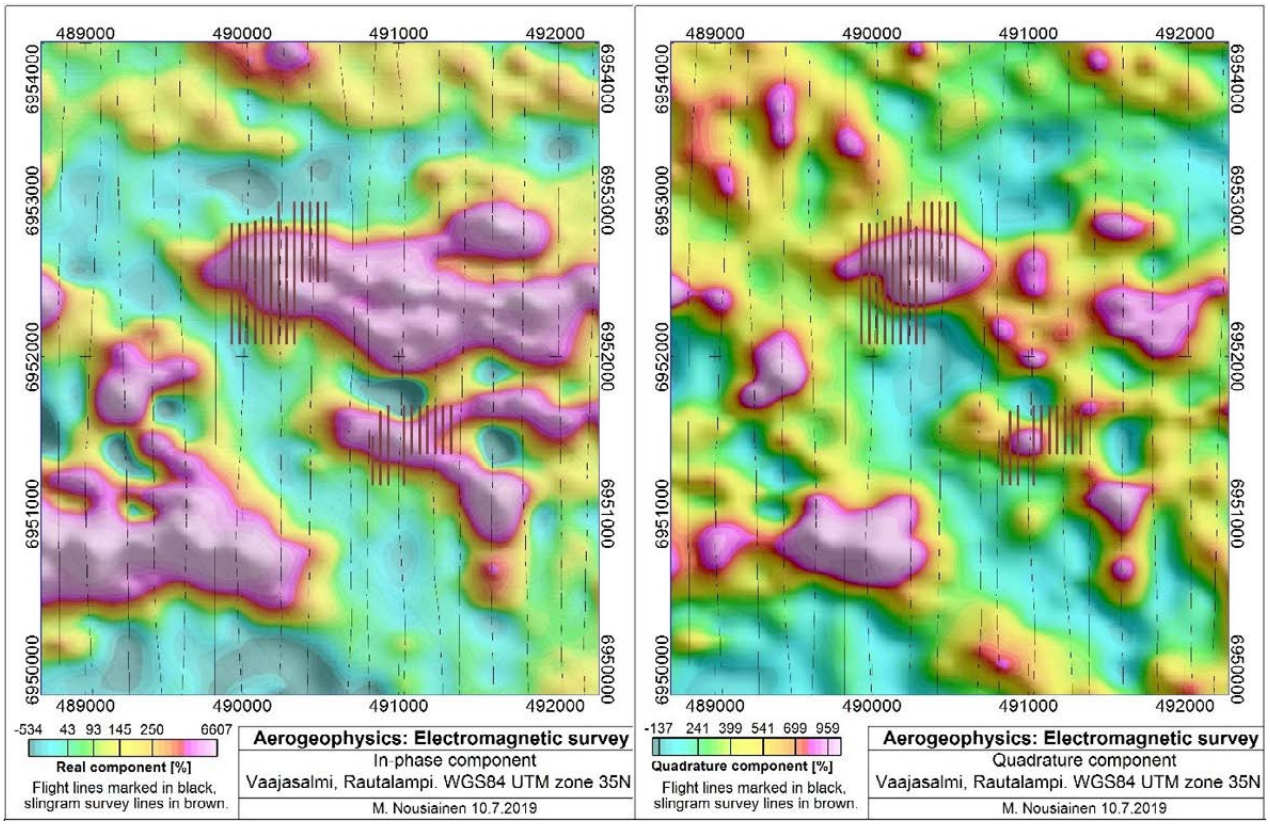

Fig. 6. Electromagnetic data from the low-altitude aerogeophysical survey by GTK. The high values of the in-phase component (on the left) are related to good subsurface conductors. The high values of the quadrature component are related to weak conductors such as wetlands. Geophysical map from aerogeophysical data, Bedrock of Finland – DigiKP.

3.2.1 Magnetic survey results

A magnetic survey was conducted between 31 October and 22 November 2017. The instruments used were a GSM19W Overhauser magnetometer as a rover and a Scintrex Envi magnetometer as a base station. The measurement frequency was 2 Hz. The data were filtered so that the point spacing was at least one meter.

Magnetic results are presented as a grid in Figure 7. In the grid, the original data are interpolated to the whole survey area. The magnetic data are reduced to pole in order to simplify the visual interpretation.

In the northern subarea, Koivuniemi, a large magnetic anomaly was detected in an east–west direction and some smaller anomalies. In the southern subarea, Saareke, anomalies were recorded in a northwest–southeast direction and a smaller anomaly near the northeast corner of the survey area.

The magnetic field survey data contain the same large-scale features as in the aeromagnetic data, but especially in the southern subarea, Saareke, the smaller features are more clearly visible in the field data.

3.2.2 Electromagnetic survey results

A slingram survey was conducted between October and November 2017. The point separation was 20 m and the coil separation (distance between the transmitter and receiver) was 100 m. Four measurement frequencies were used: 400, 800, 1700, and 3500 Hz. The original plan was to conduct slingram and magnetic surveys along the same lines, but the final slingram survey area was smaller.

Slingram results are presented as color grids in Figure 8. When inspecting the results, it is important to remember that conductors cause negative data values. In the northern of the two subareas, Koivuniemi, clear negative anomalies were detected

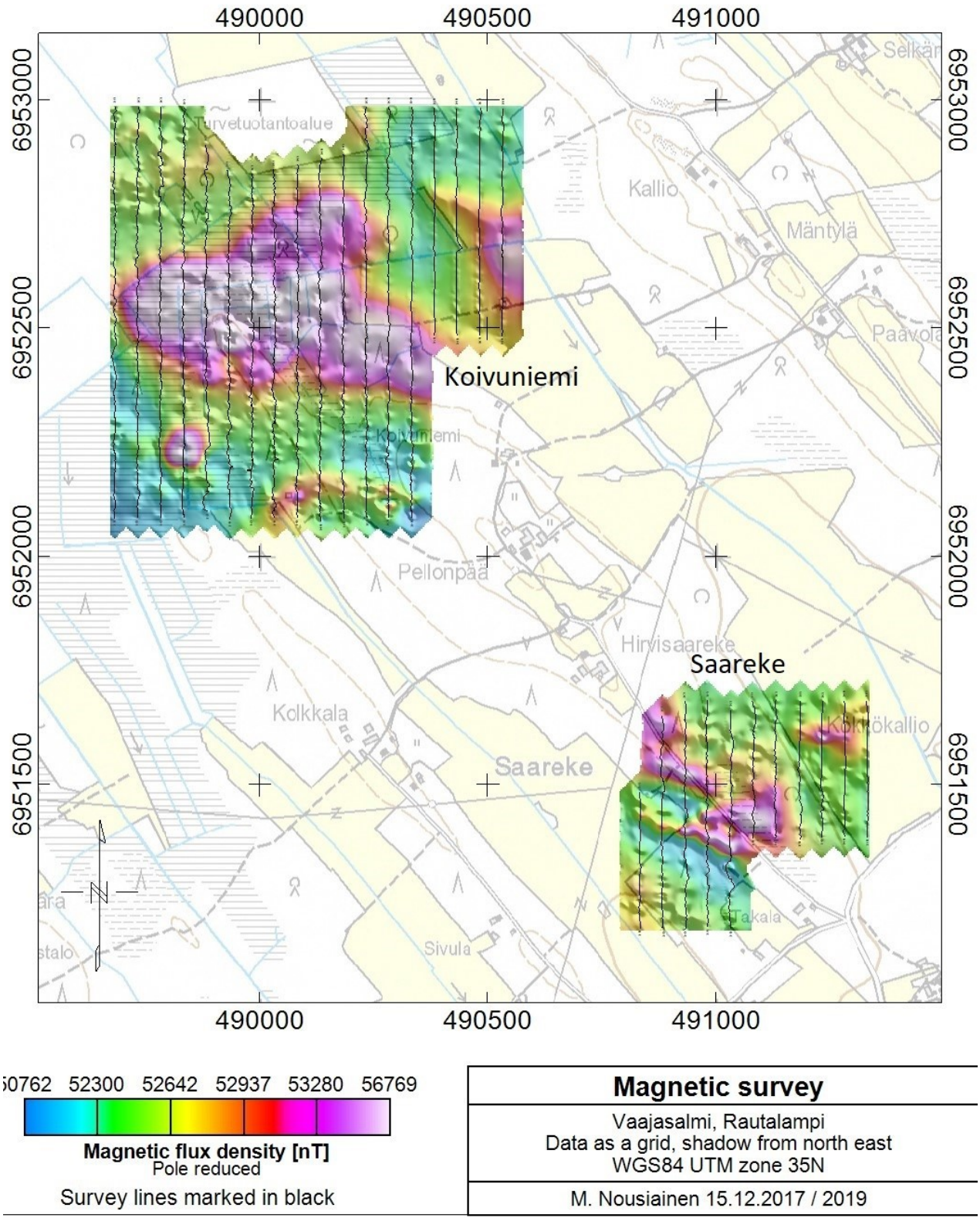

Fig. 7. Magnetic results from Vaajasalmi as a grid. Basemaps: © National Land Survey of Finland.

in the north and middle of the survey area. In the southern subarea, Saareke, a clear negative anomaly was recorded in a northwest–southeast direction, and also a weaker anomaly near the northeastern corner of the area. As expected, the conductive anomalies observed in slingram data match the airborne EM results, giving more detailed information. Airborne EM and slingram data can be used together to estimate how the most interesting features seen in slingram data continue outside the survey area.

Grids of slingram results can be used to gain a broader perspective of the study area. More detailed information from the same data are easier to absorb when the data are presented as profiles. If slingram data are used to design boreholes or construct geological models, the data should be modeled.

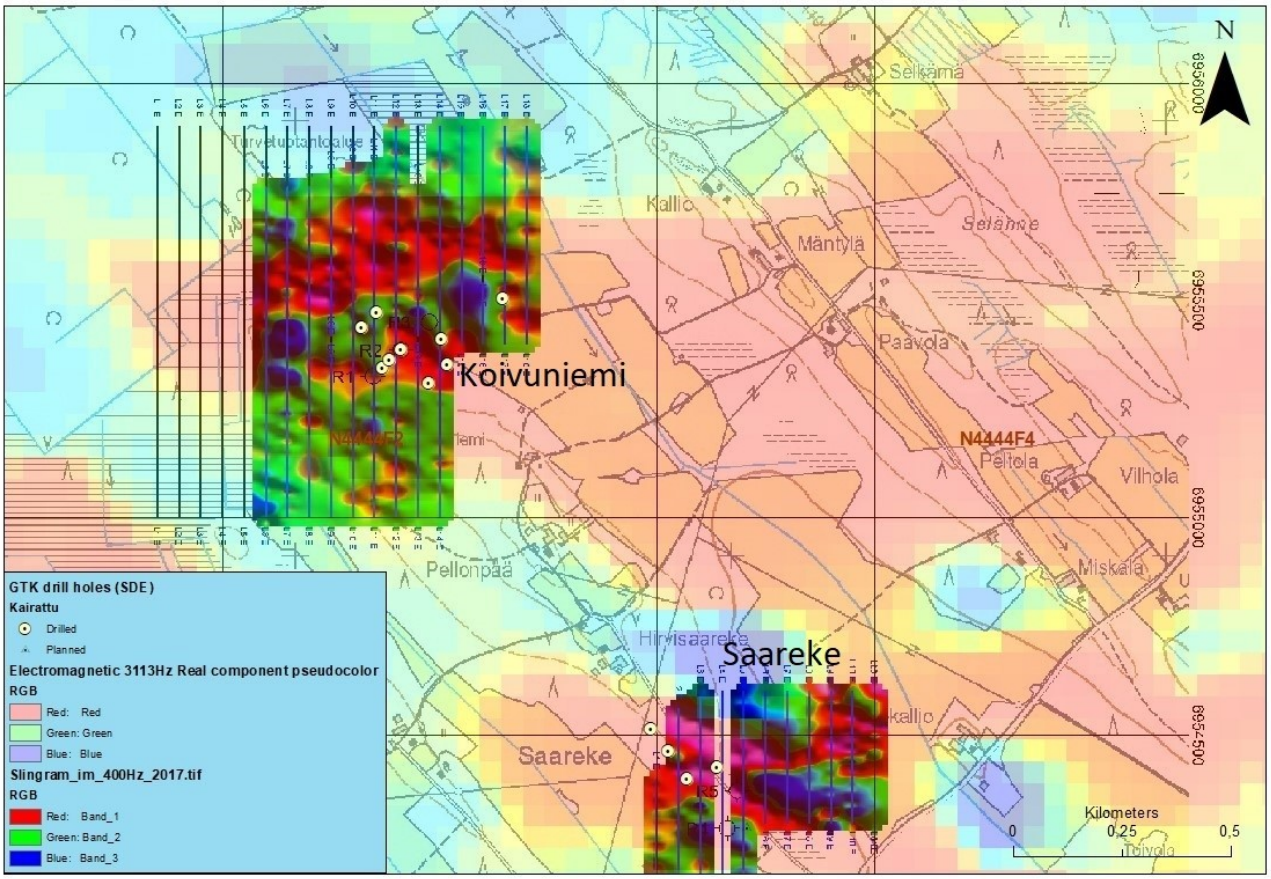

Fig. 8. Slingram im_400hz with an aerogeophysical electromagnetic 3 kHz map in the background and drill hole locations indicated. The first drilling program in Koivuniemi was conducted before ground measurement data were available. Background map from aerogeophysical maps, Bedrock of Finland – DigiKP.

3.2.3 Example of combining magnetic and slingram data

Figure 9 illustrates the combination of magnetic field survey data as a color grid and the two lowest frequencies of the slingram survey as profiles. The magnetic data presented are a tilt derivative of the original data. The tilt derivative has zero value at the ends of a magnetic body and can therefore be used to outline the sources of magnetic anomalies. Graphite is very conductive but not magnetic. Thus, if the graphite is not within another material that is magnetic, negative slingram values located outside magnetic anomalies can be sought.

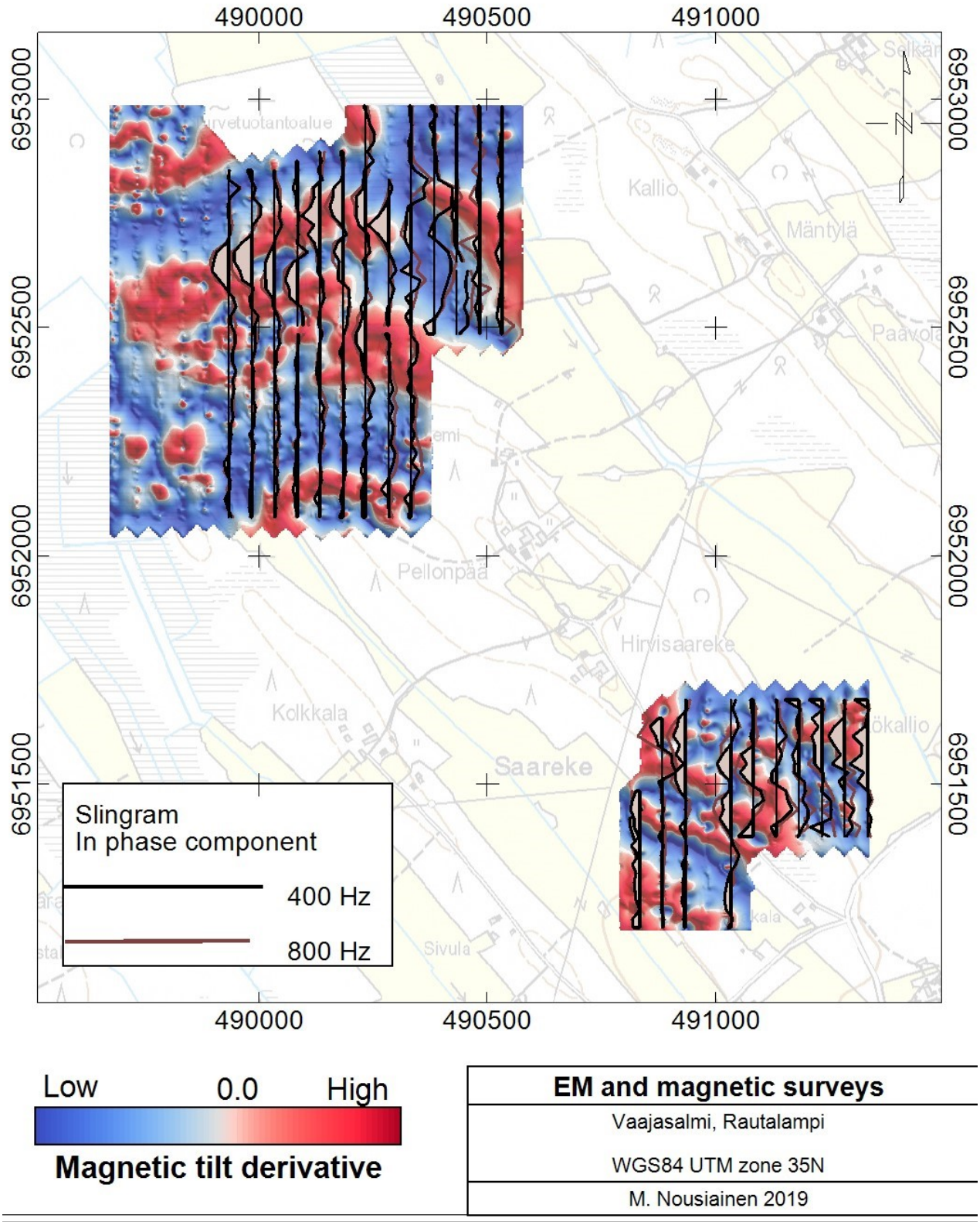

Fig. 9. Combination of magnetic and slingram data. Negative slingram values are plotted on the left side of the survey line and emphasized with a light color. Basemaps: © National Land Survey of Finland.

4 DIAMOND DRILLING & BEDROCK GEOLOGY

4.1 Koivuniemi

A drilling program in Koivuniemi comprising 9 drillholes totaling 763.20 m was planned based on the structural interpretation of aerogeophysical conductive maps. Flake graphite layers were penetrated in all drillholes that reached the bedrock, which in most places has over 10 m of overburden. The best drill intersection was in drillhole (dh) R17, with 23.55 m @ 10.6% graphitic C. The same layer was reached in the profile in drillhole R16 in front of R17, with 11 m @ 10.88% graphitic C. According to drill hole profiles R16, R17 and R22, three graphite-rich layers were intersected with a dip direction towards the SW and an angle of 50–60 degrees. Drillhole R18 reached a more intact and larger northern anomaly that continues beyond the ground measurement area to the E and W in profile C–D (Fig. 10) (Appendix 2).

The majority of the rocks in Koivuniemi are composed of intermediate volcanites (tuffites) that are highly silicified (Figs. 3 and 12). The competence contrasts between smaller graphitic layers intertwined with the silicified tuffites makes the rock incoherent for diamond drill sampling. The rock remains intact in thicker graphite sections, such as the best intersection (Fig. 11) in R17.

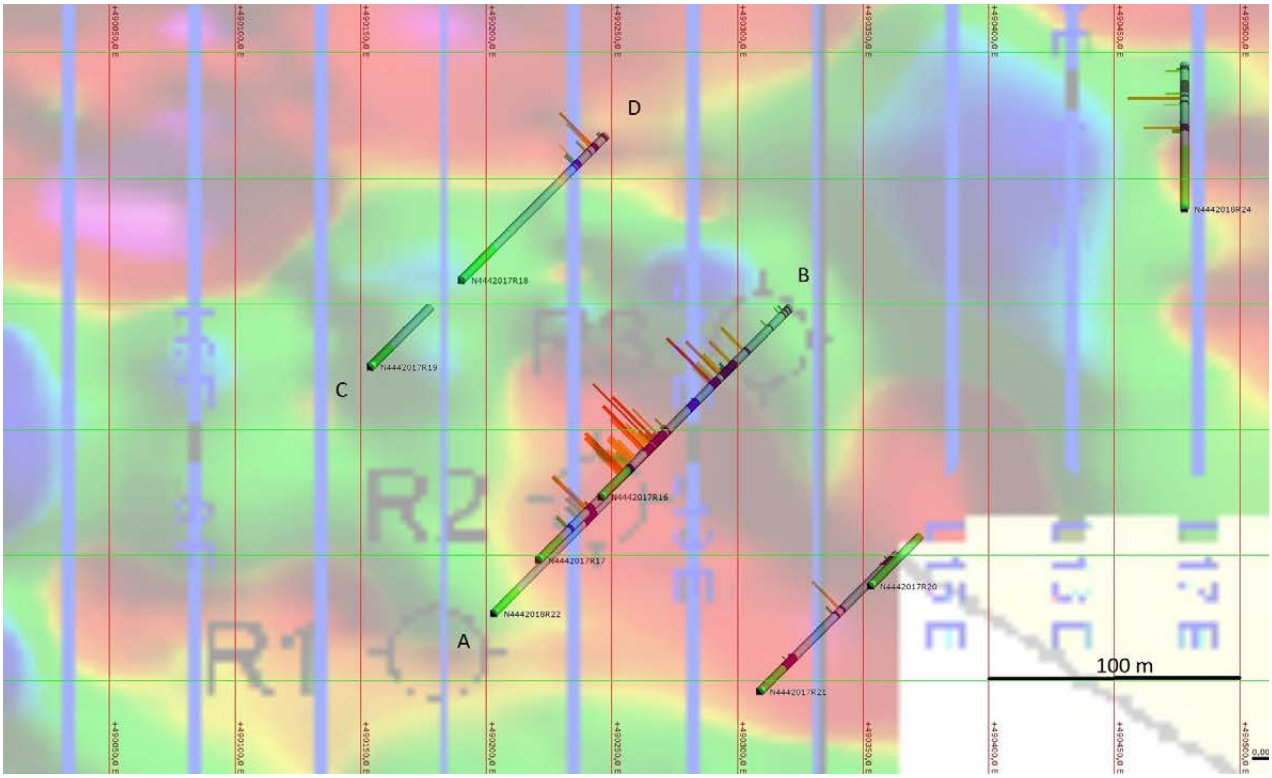

Fig. 10. Koivuniemi drill holes placed in a slingram 400 Hz background map. The ground measurement maps revealed a more precise location for a more intact conductive anomaly northwards from the performed drilling program. Drillhole R18 in profile C–D (Appendix 2) reached the northern anomaly with a high graphitic content, indicating an abundant presence of flake graphitic layers in the northern conductive anomaly.

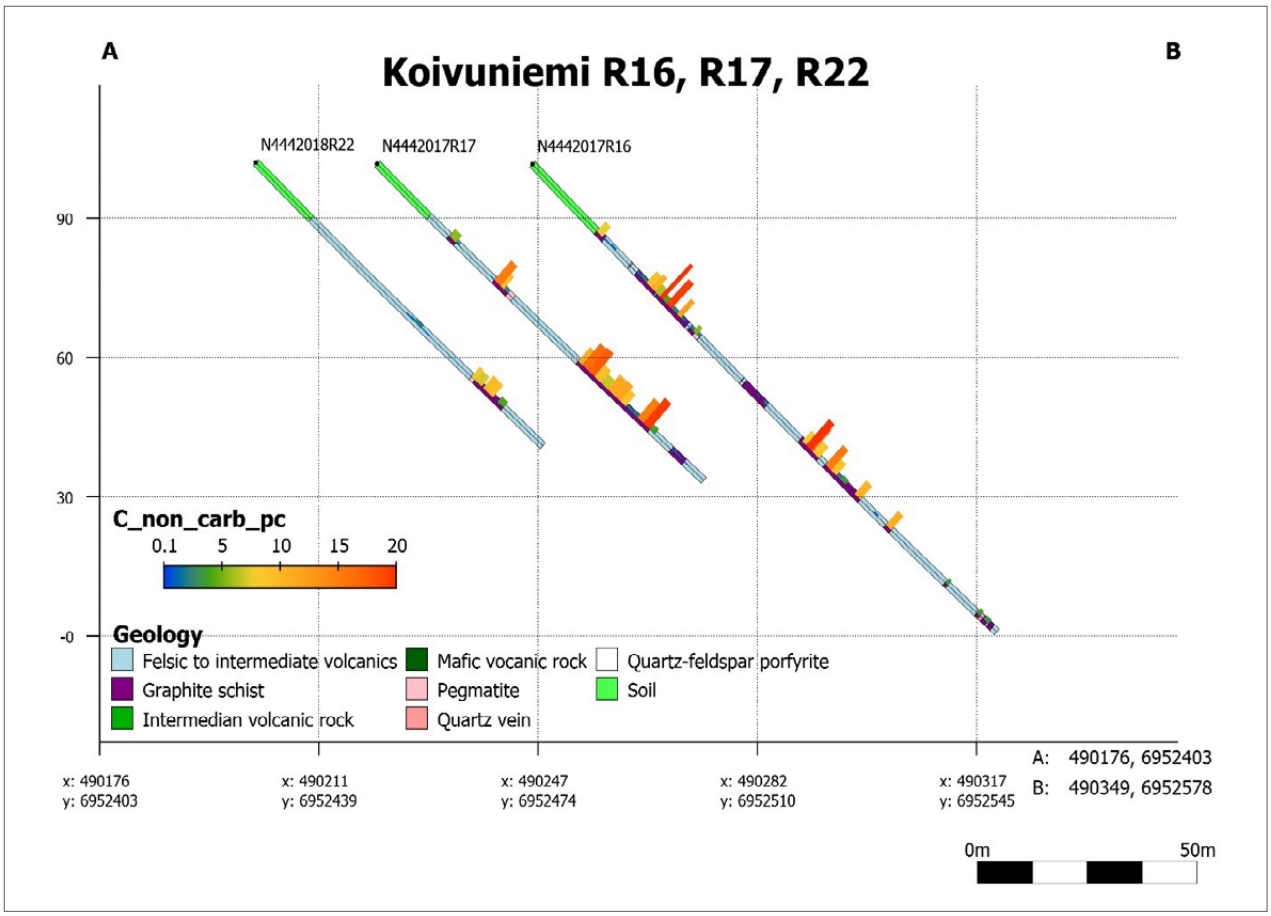

Fig. 11. Profile A–B with drillholes R16, R17, and R22.

Fig. 12. Rock contact in R17 of the darker flake graphite-rich schist and intermediate volcanic rocks.

4.2 Saareke

The Saareke target is located 1.5 km SE of Koivuniemi within the location of a separate conductive anomaly in which a small 4-drillhole program totaling 500 m was carried out in the winter of 2018. The highest graphite content in the Saareke rocks remained under 5%. The best length weighted average was 6 m @ 3.6% in drillhole R33. Besides the lower graphite content, the volcanic rocks are more of a mafic type with a large amount of hornblende present in some sections (R34, R35 & R36). These rocks have been logged as hornblende gneiss.

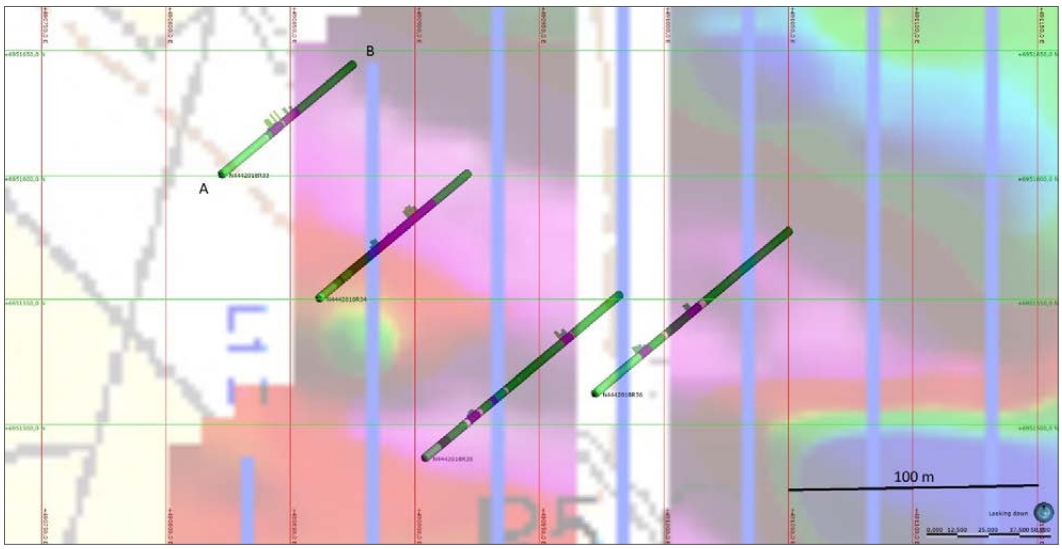

Fig. 13. The Saareke drill holes placed on a slingram 400 Hz background. The conductive anomaly does not reflect a high graphitic content, as in Koivuniemi. The anomaly may have partly been caused by the hornblende-rich volcanic rocks.

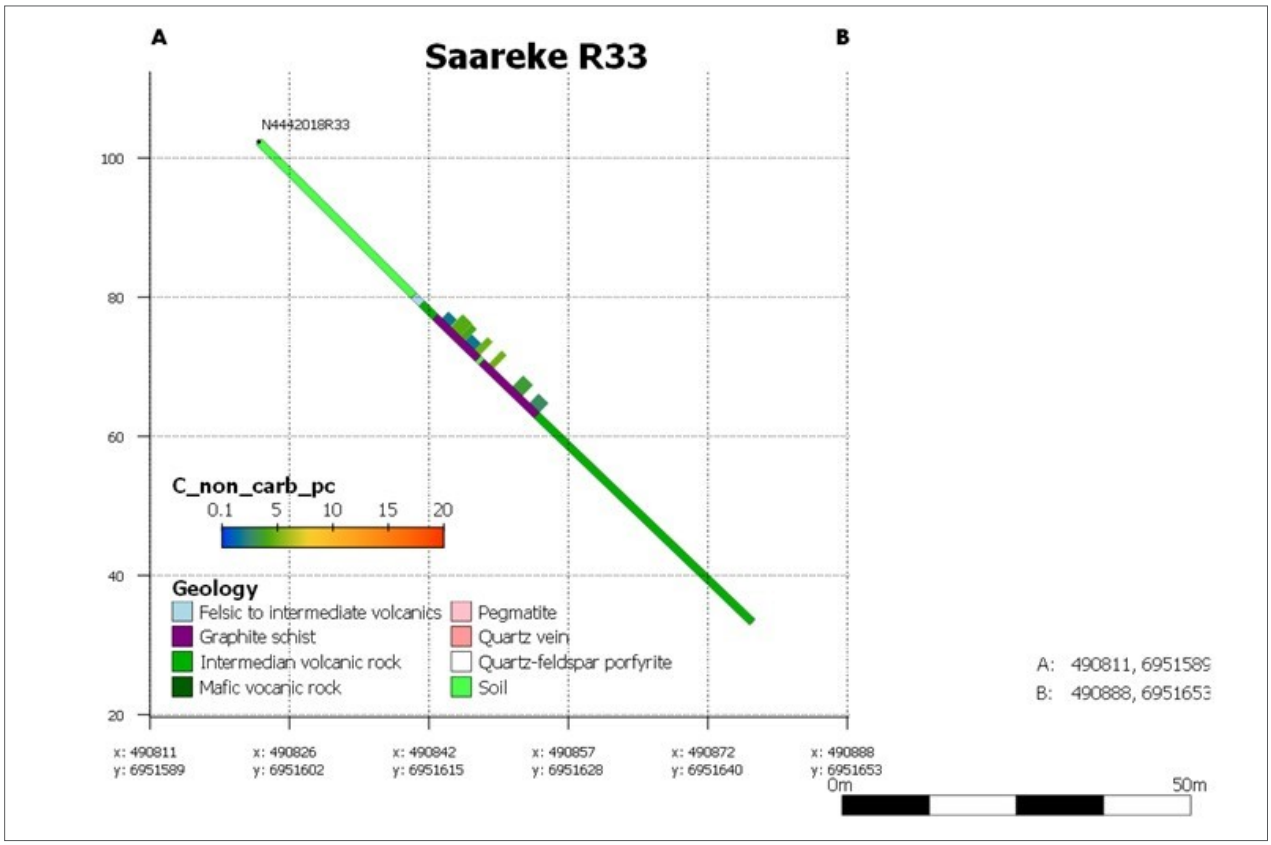

Fig. 14. Drillhole R33 in Saareke. The graphite content remained under 5% in the Saareke drill holes.

5 CHEMICAL ANALYSES

Altogether, 156 drill-core samples were analyzed, of which 109 were from the Koivuniemi and 47 from the Saareke target. The samples were analyzed by Eurofins Labtium Oy with sodium peroxide fusion as a decomposition pretreatment method (720P) and determination with ICP–OES. The C content was measured with a C analyzer after combustion pretreatment methods 811L and treatment with HCL 816L (Appendix 1).

No significant base metal mineralization was associated with the graphite-rich layers in the executed drilling programs. Tables 1 and 2 present the highest, lowest, and median values of selected elements in the Koivuniemi and Saareke targets.

Table 1. Maximum, minimum, and median values of selected elements from all samples in Koivuniemi.

Value	C%	Zn%	V%	Cu%	Co%	Ni%	Cr%	Li%	Mo%	Fe%	Ti%
Max	28.1	0.123	0.126	0.041	0.003	0.105	0.036	0.004	0.02	11.5	0.56
Min	0.05	0.005	0.005	0.002	0.001	0.005	0.003	0.001	0.005	0.01	0.01
Median	2.7	0.019	0.037	0.011	0.001	0.013	0.012	0.002	0.005	4.77	0.33

Table 2. Maximum, minimum, and median values of selected elements from all samples in Saareke.

Value	C%	Zn%	V%	Cu%	Co%	Ni%	Cr%	Li%	Mo%	Fe%	Ti%
Max	5.27	0.166	0.063	0.046	0.002	0.036	0.041	0.004	0.006	13.6	0.4
Min	0.05	0.007	0.06	0.004	0.001	0.005	0.006	0.001	0.005	2.83	0.14
Median	1.98	0.049	0.038	0.018	0.001	0.015	0.009	0.001	0.005	7.23	0.24

5.1 Element correlation plots

Correlation plots of selected base metal elements were prepared for the most graphite-rich sections (Figs. 15 and 16, Tables 3, 4, and 5). The plots illustrate that graphite is closely associated with Ni, V, and Cu in Koivuniemi. It is necessary to note that the correlation table of Koivuniemi drillhole R18 (Table 4) is only based on six of the most graphite-rich samples. The Saareke correlation plot with Cr and Zn associated with C may reflect the change in rock type analyzed (based on limited data). The four drillholes in Saareke also yielded a higher median value for Fe, which is probably related to the observed more hornblende-rich volcanics. In some places, the pyrite in Saareke had a disseminated appearance, and ten samples were tested for Au with the fire assay (Labitum methods 703 and 704), which also included Pd and Pt analysis. The fire assay results indicated no increase in the content of Au, Pd, and Pt. Co was mostly below 30 ppm in all samples from Koivuniemi and Saareke. Regarding the past exploration operations focusing on Zn, it appears according to these investigations that the Zn content is more closely related to rocks with a lower C content, such as those studied in Saareke.

Table 3. Correlation of selected elements from Koivuniemi drillholes R16 and R17.

Koivuniemi R17 section 62.50 – 86.05m + R16 36.40 – 53.30 m

	Cr_%	Fe_%	Ni_%	V_%	C_%	Zn_%	Cu_%
Cr_%	1	-0.52	0.46	0.23	0.18	0.27	-0.036
Fe_%	-0.52	1	0.033	0.47	0.31	0.41	0.44
Ni_%	0.46	0.033	1	0.82	0.77	0.36	0.71
V_%	0.23	0.47	0.82	1	0.84	0.57	0.79
C_%	0.18	0.31	0.77	0.84	1	0.28	0.72
Zn_%	0.27	0.41	0.36	0.57	0.28	1	0.36
Cu_%	-0.036	0.44	0.71	0.79	0.72	0.36	1

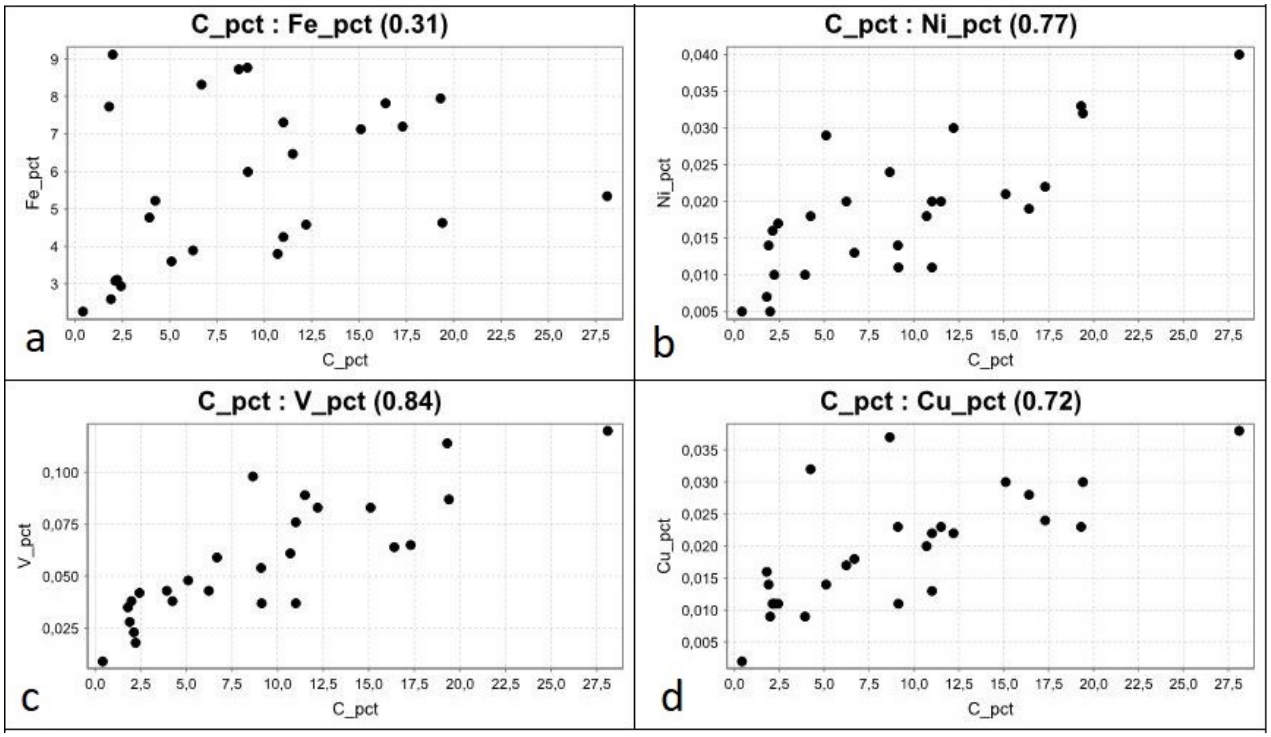

Fig. 15 a,b,c,d. Scatterplot matrix correlation of the elements C, Fe, Ni, V, and Cu presented in Table 3 from the graphite-rich layers in Koivuniemi.

Table 4. Correlation table of selected elements from Koivuniemi R18.

Koivuniemi R18 section 90.50 – 96.10 m

	Cr_%	Fe_%	Ni_%	V_%	C_%	Zn_%	Cu_%
Cr_%							
Fe_%							
Ni_%							
V_%							
C_%							
Zn_%							
Cu_%							

Table 5. Correlation matrix table from Saareke R33.

Saareke R33 section 38.20 – 44.20 m

	Cr_%	Fe_%	Ni_%	V_%	C_%	Zn_%	Cu_%
Cr_%	1	0.65	0.39	0.75	0.92	0.91	0.21
Fe_%	0.65	1	0.13	0.83	0.73	0.44	0.67
Ni_%	0.39	0.13	1	0.66	0.65	0.72	0.59
V_%	0.75	0.83	0.66	1	0.94	0.77	0.81
C_%	0.92	0.73	0.65	0.94	1	0.93	0.57
Zn_%	0.91	0.44	0.72	0.77	0.93	1	0.31
Cu_%	0.21	0.67	0.59	0.81	0.57	0.31	1

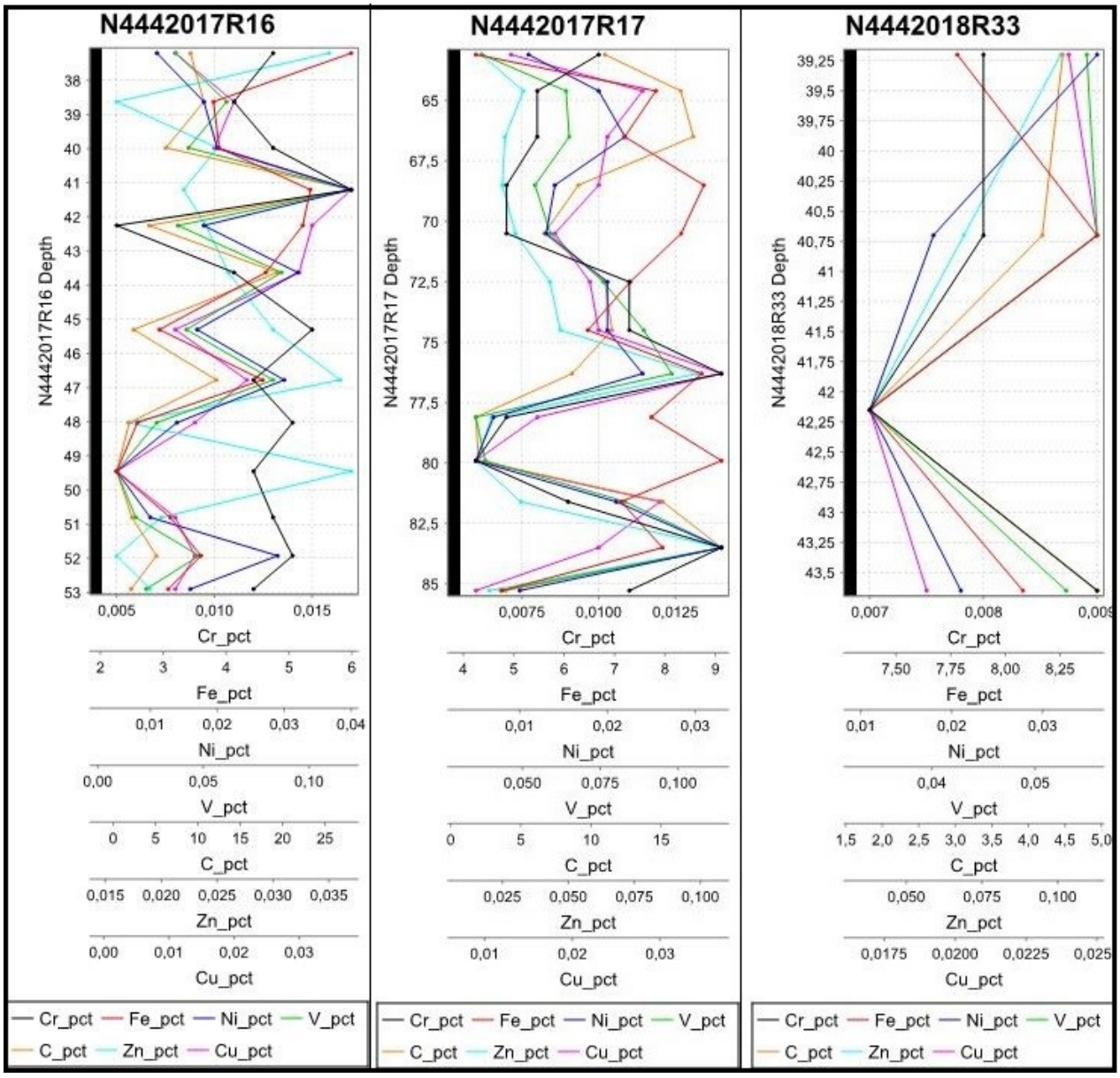

Fig. 16. Downhole correlation plots of selected elements in analyzed graphite-rich sections from drillholes R16, R17, and R33.

6 MINERALOGY

6.1 Sampling and petrographic analysis

The drill-core loggings from the research area consisted of 11 drillholes with 1178 m of drill core. A selection of 16 thin sections was prepared for petrographic and mineralogical studies from mainly metasedimentary successions. A total of 16 thin sections were prepared from mineralizations, 12 from the Koivuniemi target and 4 from the Saareke target. Petrography was investigated from the thin sections using optical microscopy. The petrographic studies aimed to define the texture and mineralogy of the graphite and associated minerals. Thin sections were studied under an ore microscope with reflected and transmitted light at variating magnifications.

6.2 Whole-rock methods

Whole-rock analyses were performed at Labtium Ltd. The carbon analyses were carried out with Labtium carbon analyzer codes 811L and 816L.

6.3 Scanning electron microscope methods

Scanning electron microscopes (SEM) were used to complement the petrographic studies and analyze the carbon concentration in graphite grains. The equipment used was an Apreo FE-SEM + EDS in the Department of Physics, University of Turku, and additional work was performed with a Phenom XL, Thermofisher, in the Department of Geology of Åbo Akademi. SEM-EDS (energy-dispersive spectrometer) analyses were performed on four thin sections (N4442017R16 40.80, N4442017R18 32.30, N4442018R24 44.75, and N4442018R34 54.55) selected to represent different textures. A low vacuum drive (LoVac, 100Pa, H2O) was used in SEM analysis, and carbon coating was not therefore needed. The O contents were omitted from analysis results.

6.4 Description of results

The selected specimens mainly consist of foliated metasediments. In the studied specimens, oriented biotite and graphite are the clear indicators of foliation. Typical major minerals in the studied specimens are quartz, plagioclase, K-feldspar, and biotite, which are associated with graphite flakes. Graphite modal amounts vary between 1% and 25%, estimated using an optical microscope. Other opaque minerals found in the thin sections are pyrite and pyrrhotite in relatively high concentrations, and chalcopyrite, sphalerite and rutile are additionally found in trace amounts. In general, the grain size varies from fine to coarse and the graphite grain size correlates with the surrounding minerals. The graphite grains appear as angular, plate-like crystals and as swirly nodule-like aggregates in mica-rich schists and more coarse-grained gneissic variates. The graphite flakes typically appear along the boundaries of the other minerals and are commonly arranged parallel to other oriented minerals, especially biotite. In the studied thin sections, the longest axis of graphite flakes varies from 50 µm to 1000 µm.

Quartz grains are typically anhedral, granular, and show features of recrystallization, with a mosaic texture, undulating distinction, and elongated grains and clusters. The grains appear in all thin sections, and coarse-grained quartz clusters with signs of recrystallization appear to be associated with the coarsest graphite flakes.

Biotite grains are found in all thin sections with widely varying modal amounts and grain sizes. Typically, biotite grains are tabular, subhedral grains (longest axis 2000 µm) and the grains are often associated with graphite and sulfide.

Plagioclase grains are common minerals in the specimens occurring as eu- and subhedral grains (100–1500 µm in diameter). The K-feldspar grains are found as non-altered sub-angular grains (500–1500 µm in diameter), and sporadically as microcline with cross-hatched twinning. Both feldspars are typically moderately altered to sericite in most

thin sections through hydrothermal alteration or sericitization. Altered feldspar clusters are associated with the largest graphite flakes.

Sulfides appear in all studied thin section with pyrite as the most dominant. The pyrite appears in groundmass as well as vein-like fillings. Individual grains are oriented parallel to the foliation of the rocks. Pyrite grains are often associated with graphite and biotite, as they form parallel orientations. Occasionally, graphite flakes appear to be cutting pyrite grains and joint fillings, indicating later crystallization. Pyrrhotite can be found as the dominant sulfide in one specimen (N4442017R17 76.70). It occurs in the groundmass parallel to foliation and as joint filling, like pyrite. Chalcopyrite and sphalerite are common minerals, but their modal amounts are minor, as they are found as small inclusions or associated with pyrite. In some of the thin sections, euhedral rutile with lamellar twinning is found in grains oriented parallel to foliation.

Table 6. Samples listed with mineralogy, estimated modal amounts of typical opaque minerals, and carbon contents from whole-rock analysis.

Locality	Analysis number	Main gangue minerals	Accessory minerals	Graphite (modal amount, %)	Py (modal amount, %)	Carbon 811L (%)	C carb 816L (%)	C non carb 816L (%)
Koivuniemi	N4442017R16 40.70-41.70	Qtz, Bt, Plag		25	10	28.1	1.49	26.6
Koivuniemi	N4442017R16 68.40-69.40	Qtz, Bt, Plag, Sil	Rt	<1	4	0.3	<0.05	0.26
Koivuniemi	N4442017R16 89.00-91.00	Qtz, Plag, Bt	Rt, Ms	10	15	8.45	<0.05	8.59
Koivuniemi	N4442017R17 36.55-38.55	Qtz, Plag, Bt	Rt, Ms	20	10	15.5	0.19	15.3
Koivuniemi	N4442017R17 75.50-77.10	Qtz, Bt, Plag, Sil	Ms	10		8.65	<0.05	8.92
Koivuniemi	N4442017R18 (Analyse not found)	Qtz, Bt, Mc, Plag	Ms, Grt	3	2			
Koivuniemi	N4442017R18 94.80-96.10	Qtz, Plag, Bt		25	10	15.8	0.53	15.3
Koivuniemi	N4442017R21 19.15-21.15	Qtz, Plag, Bt, Mc	Grt, Zrn, Ap	1	4	0.82	<0.05	0.79
Koivuniemi	N4442017R21 43.65-45.65	Qtz, Plag, Bt, Mc	Zrn	1	9	0.55	<0.05	0.51
Koivuniemi	N4442017R21 64.00-65.60	Qtz, Bt, Plag		15	10	12.8	0.1	12.7
Koivuniemi	N4442018R22 71.00-72.60	Qtz, Plag, Bt, Ms		15	15	9.55	<0.05	9.54
Koivuniemi	N4442018R24 44.75-46.30	Plag, Qtz, Bt	Zrn	20	10	12.8	<0.05	12.9
Saareke	N4442018R33 38.20-40.20	Qtz, Plag, Bt, Hbl		7	12	4.47	0.07	4.4
Saareke	N4442018R34 52.80-54.70	Qtz, Plag, Bt, Aug, Chl		5	15	1.69	0.12	1.58
Saareke	N4442018R34 69.80-71.70	Qtz, Plag, Bt	Cb	6	22	4.47	0.49	3.98
Saareke	N4442018R35 37.00-38.70	Qtz, Plag, Bt, Hbl		5	15	2.54	0.21	2.33

Abbreviations: Qtz-Quartz, Bt-Biotite, Plag-Plagioclase, Sil-Sillimanite, Mc-Microcline, Hbl-Hornblende, Aug-Augite, Chl-Chlorite, Ms-Muscovite, Grt-Garnet, Zrn-Zircon, Ap-Apatite, Cb-Carbonate, Rt-Rutile, Py-Pyrite, Po-Pyrrhotite

6.5 Detailed petrographic observations

The graphite appears in various types through the studied thin sections. These include: 1) small (<500 µm) and narrow lath-like grains in foliated rock with a rather even distribution over the specimen, 2) large (500–1000 µm), long, and plate-like flakes typically associated with quartz or feldspar clusters or major biotite stacks, 3) moderate-sized (~500 µm) grains forming joint fillings, and 4) swirly graphite accumulations. In the three latter types, the graphite is possibly partially or fully remobilized due to partial melting.

Sample: N4442017R16 40.80

Macroscopically, the sample is medium to coarse-grained, weakly foliated, and contains a major amount of graphite and sulfides. Under the microscope, the exact mineralogy consists of quartz, biotite, and plagioclase as gangue minerals (Fig. 17). Quartz grains are significantly larger than the grains of biotite and plagioclase. The amount of graphite in this sample is the highest of the studied thin sections and the flakes range from 500 to 1000 µm in length. The coarse graphite flakes are typically associated with quartz grains that show features of a grain boundary migration type of recrystallization, due to an undulating distinction and mosaic texture. Smaller graphite flakes (100–500 µm) are found as accumulations between coarser quartz aggregates and in joint fillings, indicating remobilization via shear textures, formed between schistose layers. In joints, graphite is accompanied by fine-grained quartz, biotite, and sericite.

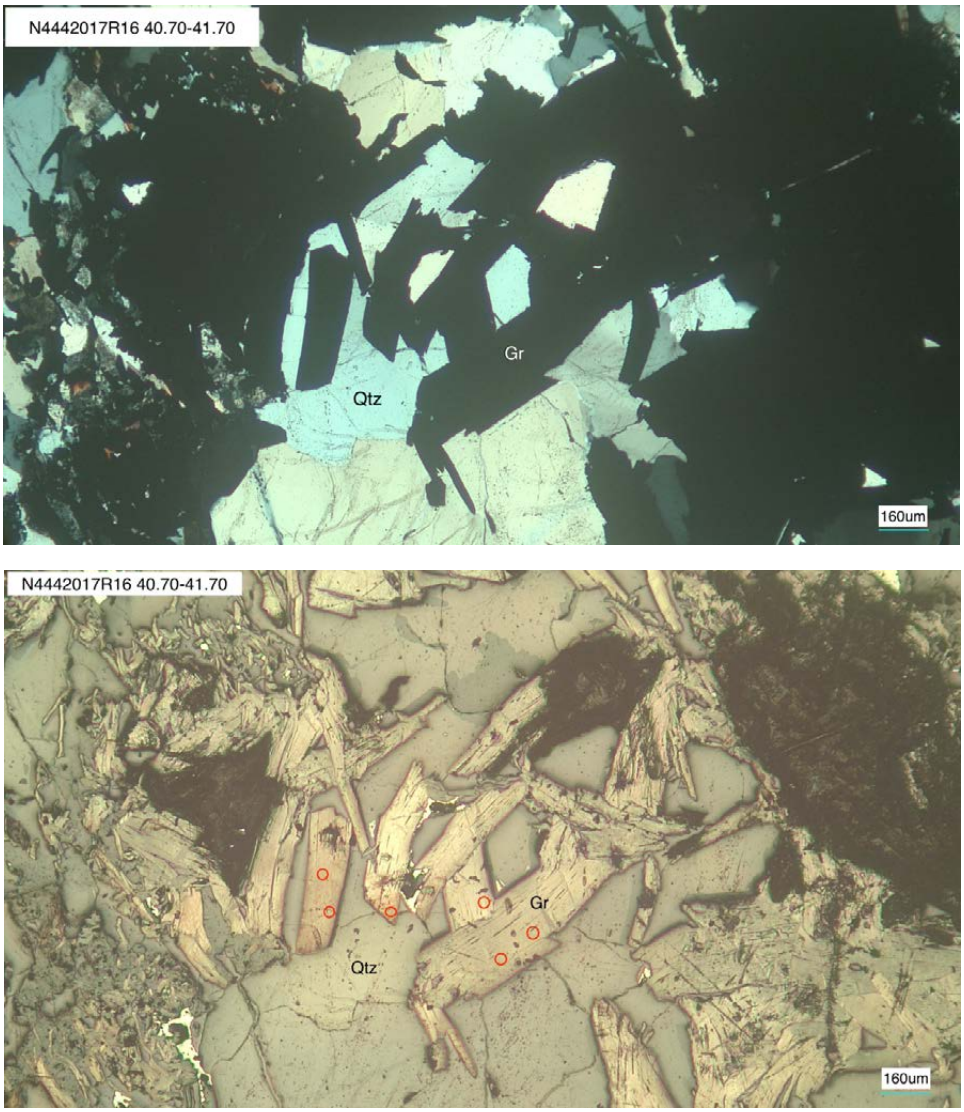

Fig. 17. Graphite in sample N4442017R16 40.80 in a cross-polarized image (above) and a reflected light image (below). Large graphite flakes are associated with quartz clusters. Red circles indicate SEM-EDS analysis spots.

Sample: N4442017R18 32.30

The studied thin section shows a lower modal amount of graphite compared to the previous sample (N4442017R16 40.80), a strongly schistose fabric with compositional layers, and more even grained between the major minerals. Quartz, biotite, K-feldspar, and plagioclase are the most abundant minerals. Accessory minerals include garnet porphyroblasts, zircon inclusions in biotite, and muscovite. Graphite and pyrite are the opaque minerals found in the specimen. Graphite flakes are oriented parallel to the foliation, the flakes are narrow and lath-like, and the volume of flakes varies between layers, with biotite-rich layers appearing most strongly associated with graphite in this thin section (Fig. 18). The tabular biotite-rich layers located between quartz- and feldspar-rich layers show a higher modal amount of graphite

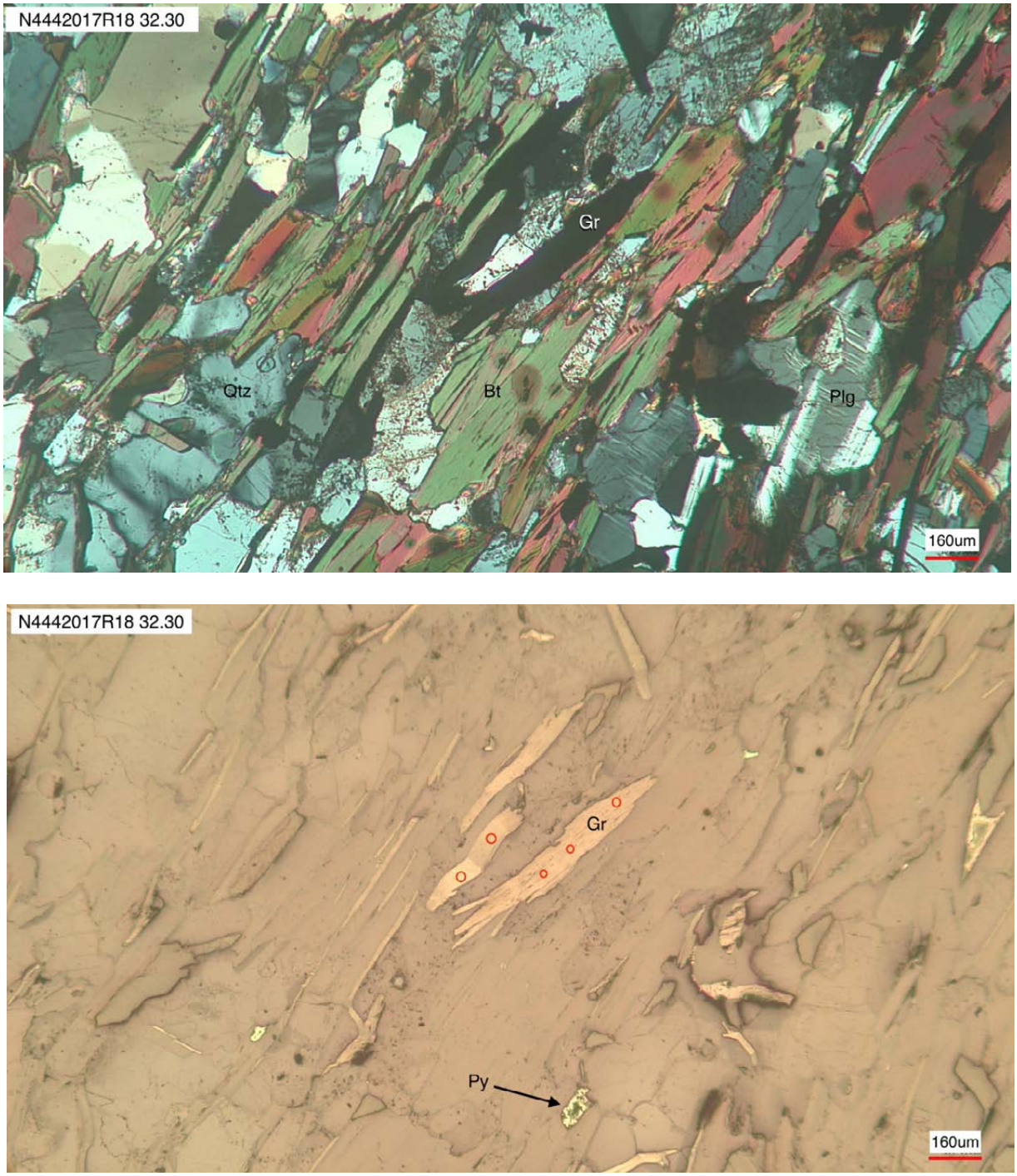

Fig. 18. Photomicrographs illustrating the appearance of graphite in sample N4442017R18 32.30: a cross-polarized image (above) and a reflected light image (below). Graphite grains are oriented parallel to foliation and often associated with biotite-rich layers. Red circles indicate SEM-EDS analysis spots.

Sample: N4442018R24 44.75

This medium to coarse-grained migmatite specimen shows a strong deformational overprint. The grain size varies from 10 micrometers to the millimeter scale in diameter. Coarse-grained parts of the rock display an igneous looking texture with large feldspar and quartz grains (>2 mm in diameter). Both feldspars are strongly altered to sericite, and a saussurite-filled joint cuts the thin section diagonally. Clear signs of partial melting are observed, as graphite and biotite form swirly textures through the thin section. Quartz grains are partly recrystallized, showing undulating extinction and a mosaic texture. The graphite occurs as large flakes (length 500 µm) inside and on the borders of sericite and quartz (Fig. 19), which is a similar feature to sample N4442017R16 40.80. A swirly graphite-biotite mass between coarse igneous-like areas appears partially melted and remobilized.

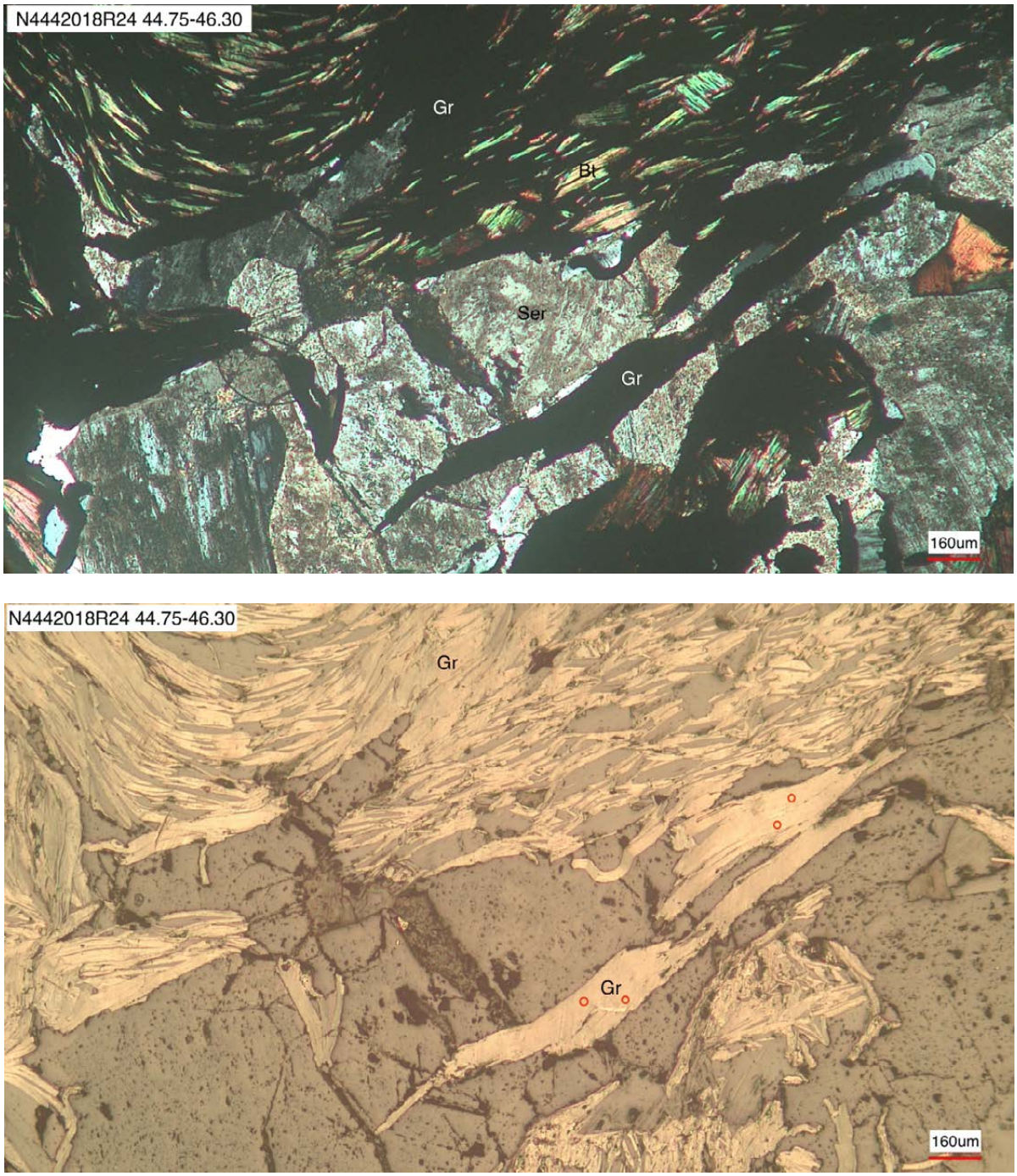

Fig. 19. Photomicrographs illustrating the features of graphite appearing as large flakes associated with sericite and biotite in sample N4442018R24 44.75: a cross-polarized light image (above) and a reflected light image (below). SEM-EDS analysis spots are marked with red circles.

Sample: N4442018R34 54.55

This sample is more fine-grained and represents layered turbiditic metasediment. The layered texture shows mineralogical variation between more felsic layers containing quartz, biotite, and sericite, and more mafic layers consisting of sericite altered plagioclase, pyroxenes, chlorite, and hornblende. The felsic layers show a schistose fabric and tabular biotite grains are parallel to narrow and lath-like graphite flakes. Quartz can be found as a ribbon-like elongated texture. The graphite flakes are evenly distributed through the thin section, although a minor increase in the amount is observed along the pyrite vein cutting the specimen. The graphite shows a clear orientation in felsic layers compared to more mafic layers. In the latter, graphite flakes are disoriented, and swirly, noodle-like graphite aggregates are common (Fig. 20). The size of the graphite flakes is visibly smaller compared to the three specimens described earlier, as on average the length of the grains ranges between 10 µm and 400 µm. Pyrite appears in two types: 1) disseminated, euhedral, cubic crystals through the thin section and 2) remobilized, massive filling in the joint between two layers. The other opaque minerals in the specimen are chalcopyrite as inclusions in pyrite and sphalerite in the edges of the pyrite vein.

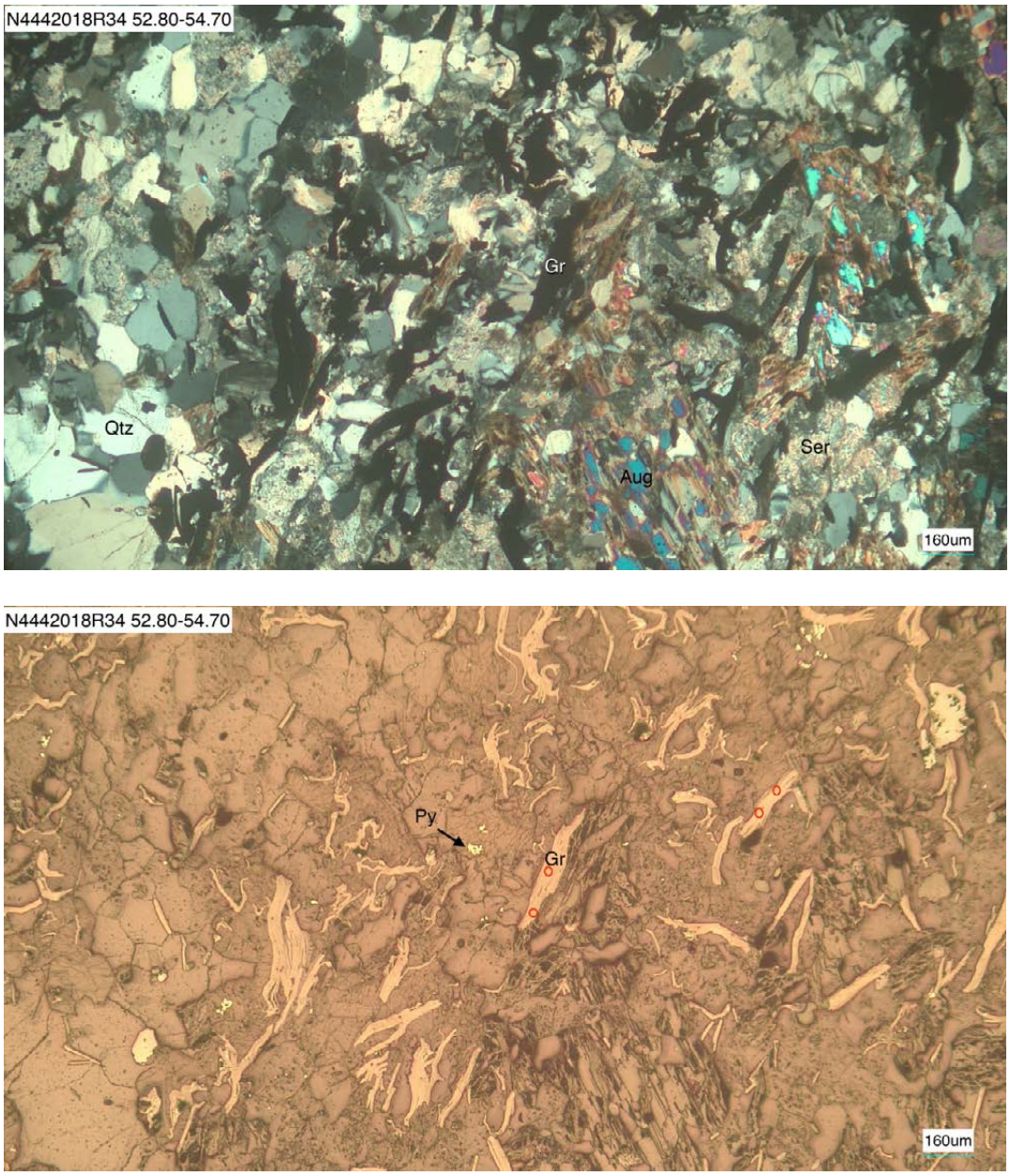

Fig. 20. Photomicrographs of sample N4442018R34 54.55: a cross-polarized light image (above) and a reflected light image (below). Graphite appears as foliation-oriented, narrow, lath-like flakes and nodule-like aggregates.

6.6 SEM-EDS and whole-rock analyses

Four thin sections were selected for the SEM-EDS analyses based on these differences, partially representing the four appearance types of graphite flakes described in the petrography sections. The aim was to measure the possible differences between the types (Appendix 3), as well as to examine the whole rock carbon contents (Table 6).

Sample: N4442017R16 40.80

SEM-EDS analyses of large flakes associated with quartz clusters presented in Figure 1 yielded a high carbon content that varied from 98.06 to 98.92 wt% (Appendix 4), and Si was the only other element above the limit of detection in the flakes. The analysis spots were taken from graphites representing petrographic type 2, the largest long plate-like flakes, associated with feldspar clusters. The non-organic carbon content for this whole rock sample was 26.6 wt%, which was the highest carbon value obtained in the study.

Sample: N4442017R18 32.30

Based on SEM-EDS analyses, the carbon content ranged from 97.58 to 97.76 wt% in analyzed flakes of this sample (Fig. 18). The analyzed flakes were small lath-like flakes and represented petrographic type 1. The remaining analyses (Appendix 4) revealed minor amounts of Na, Mg, Al, Si, K, and Fe (max total 2.42 wt%). Unfortunately, the dataset did not contain a whole-rock analysis from this sample.

Sample: N4442018R24 44.75

The graphite flakes from the sample in Figure 19 contained 98.0–98.84 wt% of carbon (Appendix 4) and low amounts of impurities such as Na, Al, Si, Fe, and Mg. The analyzed spot represented a wide range of petrographic types, from types 2–4. Several graphite minerals probably contained older inclusions of other rock-forming mineral grains. The non-organic carbon content of the sample was 12.90 wt% (Table 6).

Sample: 4442018R34 54.55

The carbon content of the SEM-EDS-analyzed graphite grains displayed in Figure 20 ranged from 97.09 to 97.7 wt% (Appendix 4). Low amounts of Fe, Al, Si, Mg, and Ca were found in the analyses. This was probably due to remnants from surrounding pyroxene and sericite-altered feldspars inside graphite flakes. The analyzed flakes represented type 1 (small and narrow lath-like grains) and type 4 (swirly nodule-like aggregates). The non-organic carbon content in this sample was 1.58 wt%, which also complements the petrographic observations of the modal amount.

6.7 Summary of mineralogy

The graphite carbon content and size of the graphite flakes are the main variables when monitoring the economic potential of graphite-bearing rocks. According to the whole-rock composition, the carbon grade of the studied samples varied from 0.26 to 26.6 wt%. The data complement the petrographic studies, in which the modal amount of graphite was estimated to range from 1 to 25%. The amount of carbon in SEM-EDS analyses of the graphite flakes was relatively high, varying from 97.1 to 98.9 wt%, and the purest graphite composition was recorded from the largest flakes.

The graphite flakes are typically aligned in parallel to general foliation and they are particularly associated with quartz and feldspar mineral clusters and biotite. The largest flakes are found in the vicinity of the quartz and sericite-altered feldspar clusters. Quartz grains are often recrystallized, and graphite flakes have possibly crystallized bordering the reformed mosaic-like grain boundaries (Fig. 16). The extinction in these quartz grains is undulating and even chessboard-like, suggesting at least grain boundary migration recrystallization temperatures of ca. 550 °C when quartz recrystallized (Stipp et al. 2002). Moderately altered plagioclases and K-feldspars are typical observations in thin sections, indicating hydrothermal activity. Large graphite flakes are associated with remobilized-looking, swirly, medium-sized flakes appearing with biotite.

Impurities inside the graphite flakes typically contain the same elements as the minerals surrounding graphite. Graphite remobilization is a likely process, based on the texture. Deformational localities that have been later filled with graphite, and the small impurities might be derived from micro-inclusions inside graphite flakes. In SEM studies, inclusions inside graphite grains appeared

to orient in parallel to the longest axis of flakes (Fig. 21), possibly between weakly bonded graphene layers. However, due to the limitations of the resolution in SEM back-scattered electron images, it was impossible to observe very small inclusions inside graphite.

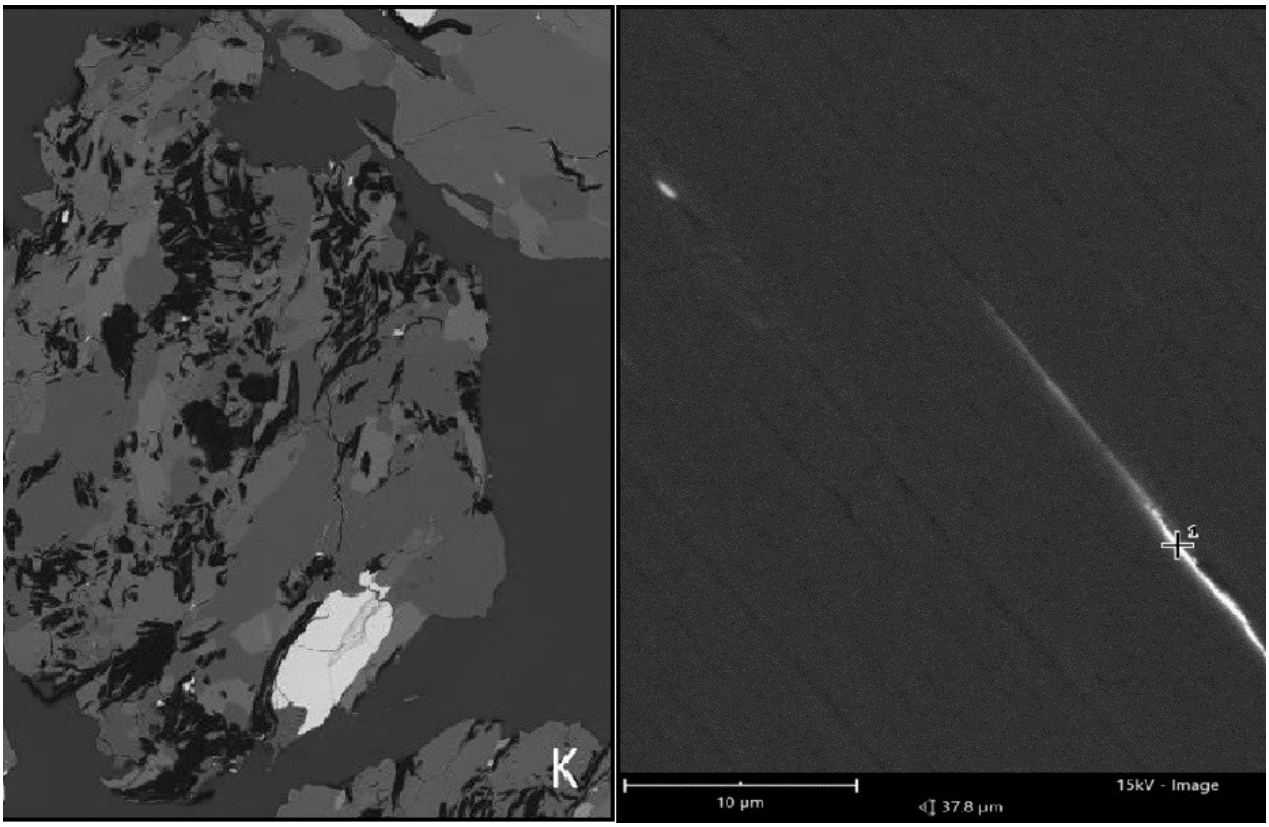

Fig. 21. *Left:* A BSE image of a grain from the Koivuniemi sample. The graphite corresponds to the darkest gray level, the intermediate gray phases are silicate minerals, and the light gray phases are S and/or Fe carrier minerals. *Right:* A typical elongated inclusion inside a graphite grain in a backscattered electron microscope image. Spot analysis of the + mark revealed elevated values of S, Fe, Si, and Al (Fig. by Jaakko Nurkkala).

7 BENEFICIATION

Testing was carried out at GTK Mintec in Outokumpu on the Koivuniemi sample. The raw material was received as drill cores at GTK Mintec in October (2020) and the tests were finalized in January (2021). The beneficiation study involved crushing, grinding, graphite concentration by flotation, and purification by alkaline roasting and acid leaching.

7.1 Sample preparation

The amount of drill core sampled from Koivuniemi was 16 kg. The drill-core samples were crushed to 100% -1.6 mm, homogenized, and split into 1-kg and 5-kg samples. A 100-g sub-sample was utilized for sieving analysis, and six size fractions were sent for chemical assays, and five for mineralogical analysis.

7.2 Analytical Methods

Chemical analyses of process products were carried out by Eurofins Labtium Oy, located in the same premises as GTK Mintec in Outokumpu. The chemical analytical methods were X-ray fluorescence (XRF) for the main elements and Eltra for C.

7.3 Methods for testing

The crushed samples were used for bench-scale flotation tests. In total, five tests were carried out on the samples. The tests started with grinding using a ball mill or rod mill. A magnetic separation stage was included in some tests after the first grinding to remove Fe and Fe-bearing minerals. The graphite was concentrated by froth flotation with a rougher stage. Regrinding of the rougher concentrate was tested to further liberate the graphite grains from gangue minerals. The rougher concentrate was then cleaned in three to four cleaning stages. The final graphite cleaner concentrate was purified by alkaline roasting and acid leaching.

7.4 Feed Samples

Table 7 presents the results of the sieving analysis and C assays. The Koivuniemi feed sample d80 was 884 µm. The highest C grade in the Koivuniemi sample was in the 75–20 µm fraction (20.6%). The C feed grade of the sample was 11.3%. This value was calculated based on the weight percentage of the size fractions.

Table 7. Koivuniemi size fractions, wt% and C grade.

		>1000 µm	1000–500 µm	500–180 µm	180–75 µm	75–20 µm	<20 µm	Feed calculated
Koivuniemi	Wt%	15.9	18.0	24.0	23.8	13.1	5.3	
	Eltra C	10.8	11.6	8.89	9.52	20.6	7.71	11.3

7.5 Flotation testing

Different flotation tests were performed to obtain information on the sample behavior in flotation, and optimize the conditions, seeking high C grades and recoveries. Table 8 details the conditions in each test performed.

The first stage of the flotation tests was grinding with a rod or ball mill. The inner dimensions of the mill were Ø190 × 220 mm, and it was charged with 8.0 kg of Fe rods or Fe balls. Grinding was performed wet, using tap water (0.9 L) at room temperature. The grinding time varied from 45 to 75 minutes.

Wet magnetic separation was carried out using a SALA magnetic separator at 0.3 T. The non-magnetic fraction was directed to froth flotation.

Flotation experiments were performed in an Outokumpu-type flotation machine (No. 3) in 2.5- or 4-liter flotation cells. In all tests, kerosene and MIBC were used. The kerosene dosage was 300 g/t in many of the tests, and the MIBC dosage was 150 g/t. In addition, Na_2SiO_3 and starch were used in some tests as depressants in the roughing stage. The tests continued with a rougher stage and three to four cleaners. The rougher concentrate was reground in most of the tests with either a rod or ball mill, and the regrinding time was 30 minutes. Figures 22 and 23 illustrate the different flowsheets tried during the test work.

Table 8. Summary of flotation tests carried out. (RM: rod mill; BM: ball mill).

Sample	Test	Grinding	Magnetic Separation	Regrinding	Rgh Flot. Dosage (g/t)		Depressants Dosage (g/t)		No. Of Cleaners
					Kerosene	MIBC	Na_2SiO_3	Starch	
Koivuniemi	K-T0	RM - 45 min	-	BM - 30 min	300	150	-	-	4
	K-T01	RM - 75 min	-	RM - 30 min	300	150	-	-	4
	K-T02	RM - 75 min	0.3 T	RM - 30 min	300	150	-	-	4
	K-T03	RM - 75 min	-	-	300	150	-	-	4
	K-T04	RM - 75 min	-	-	300	150	1500	300	4
	K-T05	RM - 75 min	-	-	300	150			4
Sample	**Test**	**Grinding**	**Magnetic Separation**	**Regrinding**	**Rgh Flot. Dosage (g/t)**		**Depressants Dosage (g/t)**		**No. Of Cleaners**
					Kerosene	**MIBC**	**Na_2SiO_3**	**Starch**	
Koivuniemi	K-T0	RM - 45 min	-	BM - 30 min	300	150	-	-	4
	K-T01	RM - 75 min	-	RM - 30 min	300	150	-	-	4
	K-T02	RM - 75 min	0.3 T	RM - 30 min	300	150	-	-	4
	K-T03	RM - 75 min	-	-	300	150	-	-	4
	K-T04	RM - 75 min	-	-	300	150	1500	300	4
	K-T05	RM - 75 min	-	-	300	150			4

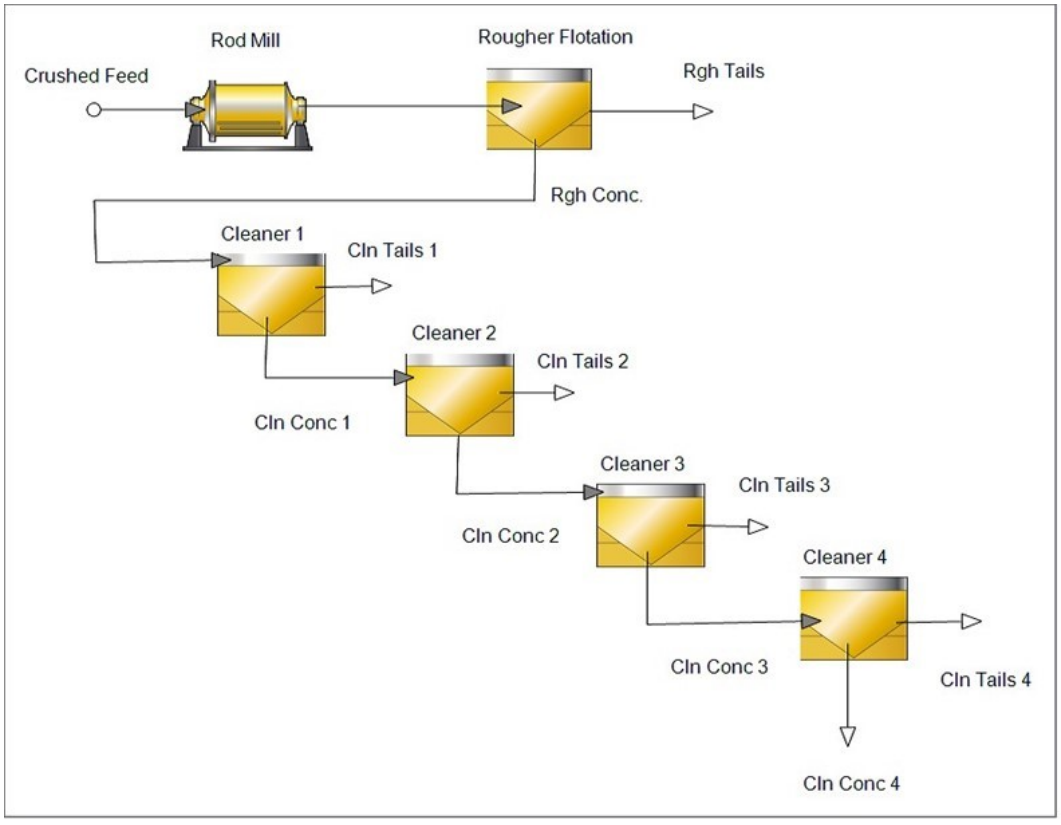

Fig. 22. Flowsheet with magnetic separation and regrinding.

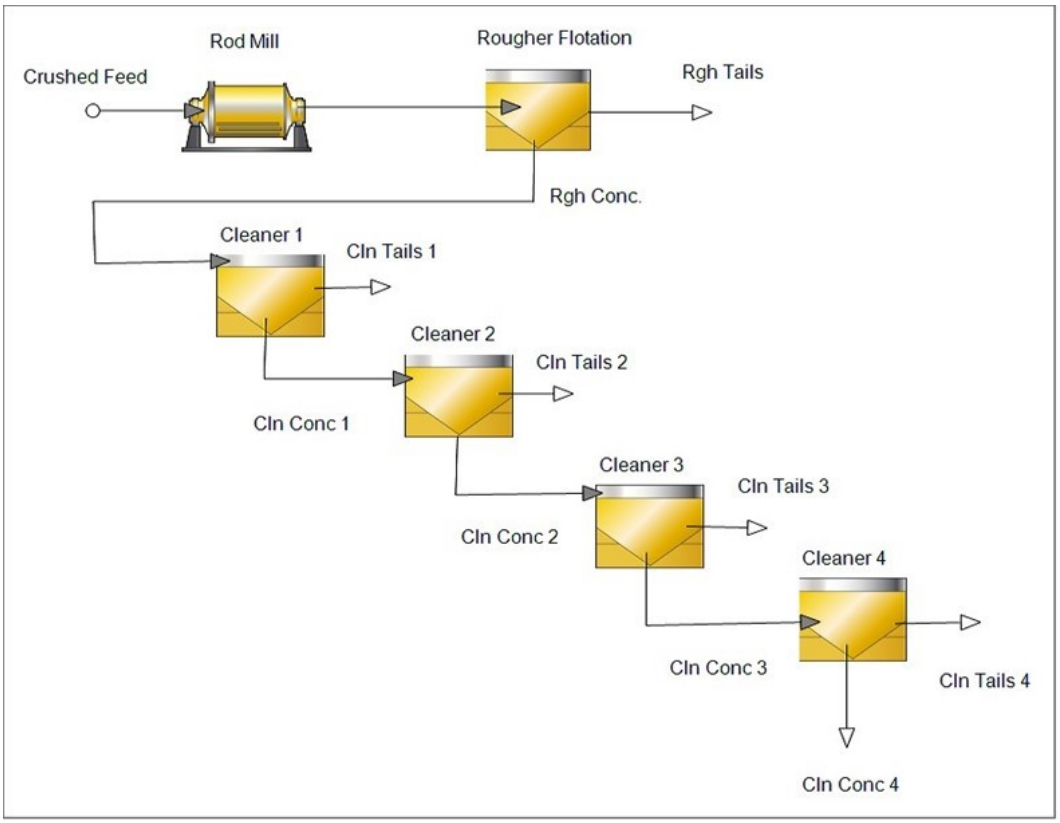

Fig. 23. Flowsheet with one grinding stage.

Considering the grinding fineness obtained in the different tests, Table 9 summarizes the grinding conditions and the d80 values. The d80 represents the fineness of the entire sample after grinding and regrinding. The d80 fineness ranged from 66 µm to 44 µm.

Table 9. Grinding conditions and d80 values for the combined sample.

Sample	Test	Grinding	Magnetic Separation	Regrinding	d 80 fineness (µm)
Koivuniemi	K-T0	RM - 45 min	-	BM - 30 min	66
	K-T01	RM - 75 min	-	RM - 30 min	44
	K-T02	RM - 75 min	0.3 T	RM - 30 min	53
	K-T03	RM - 75 min	-	-	46

Figure 24 presents the grade and recovery curves for the tests performed for each sample. In the tests conducted with a finer grinding, as in K-T01 (d8: 44 µm) compared to K-T0 (d80: 66 µm), the result was lower C recoveries and very little improvement in the C grade. In addition, the magnetic separation did not improve the C grades or recoveries in test K-T02. Contrary to the other samples tested, the one-stage grinding in K-T03 improved the C recoveries. In test K-T04 with starch and Na_2SiO3, the ore response was similar, with a slightly lower C grade and recoveries. Finally, in K-T05, the concentration of lower solids in cleaner stages (2.5 L cell instead of 1.5 L) had a positive impact on the C grade and recovery. This last test presented the best overall performance. The 4th cleaner concentrate had a C grade of 90.7%, at 81.9% recovery. The main impurity remaining was SiO_2 (3.9%). The Fe grade was 1%, and that of S 0.3%. The C losses in rougher tailings were quite low, being 1.1%.

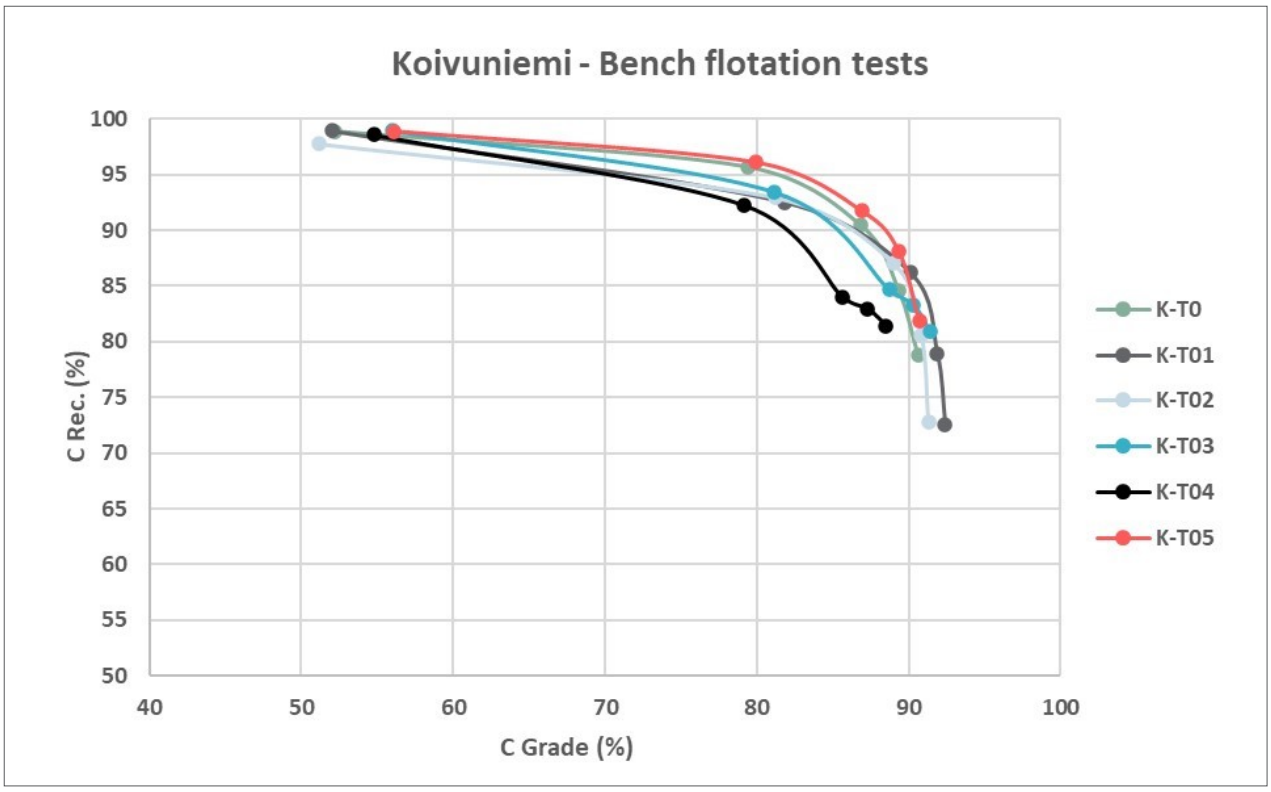

Fig. 24. The grade and recovery curves in the Koivuniemi tests.

7.6 Purification tests with alkaline roasting and acid leaching

The alkaline roasting and acid leaching tests included a first stage of alkaline roasting followed by acid leaching (Fig. 25). The test procedures were described in the article by Lu and Forssberg (2002).

In total, three purification tests were conducted on the Koivuniemi sample. Table 10 lists the purification test conditions.

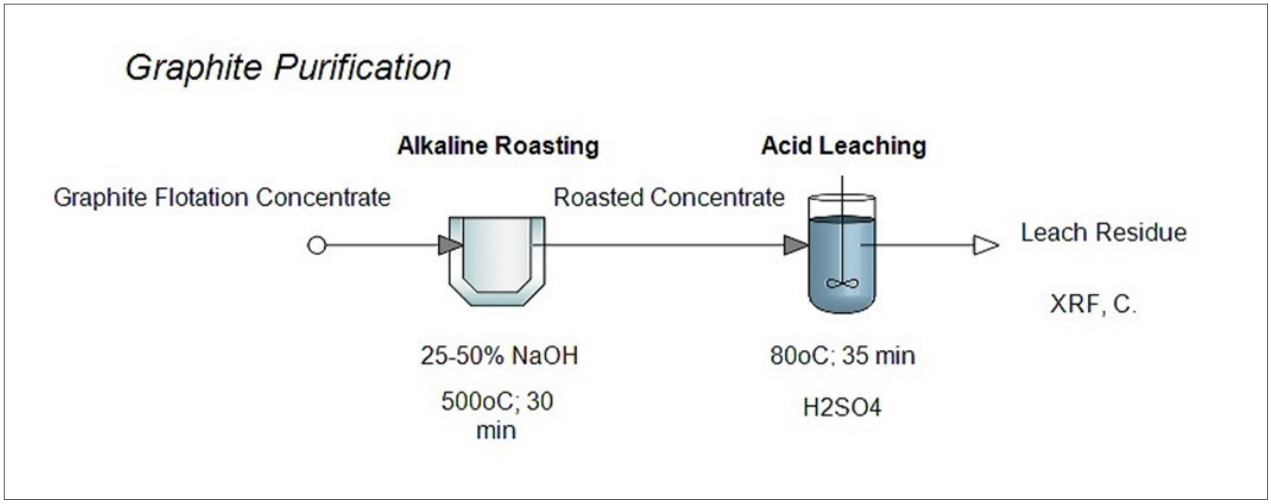

Fig. 25. Alkaline roasting and acid leaching graphite purification process.

Table 10. Koivuniemi purification test conditions.

		Roasting			Acid Leaching		
Sample	Test	NaOH Conc. (%)	T°C	Time (min)	H_2SO_4 Conc. (%)	T°C	Time (min)
Koivuniemi	K-PT1	50		30	3.9		
	K-PT2	25		30	3.9		
	K-PT3	50		30	3.9		

Table 11 presents a summary of the results. All three Koivuniemi purification tests (K-PT1, K-PT2, and K-KPT3) were able to produce a residue with over 98% C, even in the first two tests with a lower C feed grade (72.5%). The SiO_2 grade in the residue was about 0.4%, the S grade 0.007% and the Fe grade ca. 0.01%.

Table 11. Summary of the purification test results. (Res.: Residue).

Purification Test	Feed	Feed	Residue	C Upgrade	SiO_2 Feed	SiO_2 residue	S Feed	S residue	Fe Feed	Fe residue
		C (%)	C (%)	%	%	%	%	%	%	%
K-PT1	K-CP1 CC4	72.5	98.3	35.6	10.7	0.3	0.65	0.007	1.66	0.01
K-PT2	K-CP1 CC4	72.5	99.1	36.7	10.7	0.4	0.65	0.006	1.66	0.01
K-PT3	K-T05 CC4	90.7	98.3	8.4	3.9	0.4	0.31	0.007	1.02	0.01

To summarize, the measured C feed grade for the Koivuniemi sample was 11.3%. A bench-scale test including crushing, grinding, magnetic separation, and flotation gave a response to the flowsheet tested, reaching a concentrate of 91% C at 82% recovery. The purification scheme met the targeted C grade of over 99% C for the Koivuniemi sample.

8 CONCLUSIONS AND RECOMMENDATIONS

In 2017, the Geological Survey of Finland discovered a new potential flake graphite occurrence in the Vaajasalmi area in Rautalampi, which is located 3 km NE of the previously known Käpysuo graphite occurrence. The graphite potential can be seen in airborne geophysical conductive maps to continue several kilometers towards the NE, in a region characterized by large-scale structural markers. A small drilling campaign resulted in an intersection of 23.55 m @ 10.6% graphitic C in Koivuniemi. The prospectivity potential of graphite can be outlined by combining geophysical magnetic and slingram ground measurement maps to observe negative slingram values located outside magnetic anomalies. Drill hole R18 reached a more intact and larger conductive area, the so-called northern anomaly, which continues beyond the ground measurement area to the E and W. Chemical analyses revealed no significant elevation of other base metals, even though Ni, V, Cu, and Fe correlated closely with C. The rocks in Saareke are hosted by a more mafic volcanic rock type with a higher Fe and significantly lower C content. The best graphite section in Saareke was 6 m @ 3.6% graphitic C in drillhole R33. The graphite grains were studied in greater detail from 14 thin sections with the aim of describing their size, appearance, and siting in the matrix. The graphite grains appear as angular, plate-like crystals and as swirly, nodule-like aggregates in mica-rich schists and more coarse-grained gneissic variates. The graphite flakes typically appear along the boundaries of other minerals and are commonly arranged in parallel to other oriented minerals, especially biotite. In the studied thin sections, the longest axis of graphite flakes varied from 50 µm to 1000 µm.

The crushed samples were used for bench-scale flotation tests at GTK Mintec in Outokumpu. Five varied test procedures were applied to a 16-kg drill-core sample. The tests started with grinding with a ball mill or rod mill. A magnetic separation stage was included in some tests after the first grinding. Graphite was concentrated by froth flotation with a rougher stage. Regrinding of the rougher concentrate was tested in some tests. The rougher concentrate was cleaned using three to four cleaning stages. The final graphite cleaner concentrate was purified by alkaline roasting and acid leaching. The flowsheet produced a concentrate of 91% C at 82% recovery before the purification (alkaline roasting and acid leaching). The purification scheme reached a grade of over 99% for the Koivuniemi sample.

The number of applications for graphite and especially graphene is rapidly increasing. The flake size is still the most important factor if graphite is intended as an end product for the refractories industry, whereas the purity and grain shape are more vital if graphite is to be used as a battery material. Supported by good first-stage beneficiation test results, the first recommendation for future work would be to diamond drill the northern conductive anomaly, which is indicated by ground geophysical measurements.

AKNOWLEDGEMENTS

All the participants in this project are thanked for their valuable input. The mineralogical part was done in co-operation with Turku University and executed in a Master Thesis project by Jaakko Nurkkala under supervision of Prof. Esa Heilimo.

REFERENCES

Ahtola, T. & Kuusela, J. 2015. Esiselvitys Suomen grafiitti-potentiaalista. Geologian tutkimuskeskus (GTK), arkistoraportti 88/2015. 14 p. Available at: https://tupa.gtk.fi/raportti/arkisto/88_2015.pdf

Al-Ani, T., Ahtola, T. & Kuusela, J. 2018. Prospecting and exploration of flake graphite occurrences in Central and Southern Finland. Geological Survey of Finland, Open File Work Report 24/2018. 28 p. Available at: https://tupa.gtk.fi/raportti/arkisto/24_2018.pdf

Al-Ani, T., Leinonen, S., Ahtola, T. & Salvador, D. 2020. High-Grade Flake Graphite Deposits in Metamorphic Schist Belt, Central Finland – Mineralogy and Beneficiation of Graphite for Lithium-Ion Battery Applications. Minerals 10, 680.

Bedrock of Finland – DigiKP. Digital map database [Electronic resource]. Espoo: Geological Survey of Finland [referred 01.01.2018]. Version 1.0.

Hautaniemi, H., Kurimo, M., Multala, J., Leväniemi, H. & Vironmäki J. 2005. "Three in One" aerogeophysical concept of GTK in 2004. In: Airo, M.-L. (ed.) Aerogeophysics in Finland 1972-2004: Methods, System Characteristics and Applications. Geological Survey of Finland, Special Paper 39, 21–74. Available at: http://tupa.gtk.fi/julkaisu/specialpaper/sp_039_pages_021_074.pdf

Hölttä, P. & Heilimo, E. 2017. Metamorphic map of Finland. In: Nironen, M. (ed.) Bedrock of Finland at the scale 1:1 000 000 - Major stratigraphic units, metamorphism and tectonic evolution. Geological Survey of Finland, Special Paper 60, 77–128. Available at: http://tupa.gtk.fi/julkaisu/specialpaper/sp_060_pages_077_128.pdf

Koistinen, T. 1984. Kaivoslain mukainen tutkimustyöselostus "Pukkiharju" ja "Käpysuo" kaiv.rek.nro:t 2924/1 ja 3162/1. Outokumpu Oy, Valtausraportit OKU_3554. 3 p. + app. Available at: https://tupa.gtk.fi/raportti/valtaus/2924_1.pdf

Koistinen, T. & Vihreäpuu, U. 1982. Suonenjoki ja Rautalampi lentoalue I-II 1975–1982. Outokumpu Oy, OKU_432. 253 p. Available at: https://tupa.gtk.fi/raportti/arkisto/001_3223_3224_3241_3242_TJK_UMV_82.pdf

Lahtinen, R. 1994. Crustal evolution of the Svecofennian and Karelian domains during 2.1–1.79 Ga, with special emphasis on the geochemistry and origin of 1.93-1.91 Ga gneissic tonalites and associated supracrustal rocks in the Rautalampi area, central Finland. Geological Survey of Finland, Bulletin 378. 128 p. Available at: https://tupa.gtk.fi/julkaisu/bulletin/bt_378.pdf

Lu, X. J. & Forssberg, E. 2002. Preparation of high-purity and low sulphur graphite from Woxna fine graphite concentrate by alkali roasting. Miner. Eng. 2002, 15, 755–757.

Nurkkala, J. 2021. Petrography and genesis of Vaajasalmi graphite targets in Rautalampi, Central Finland. University of Turku, Unpublished MSc- thesis.

Pääjärvi, A. 2000. Rautalammin ja Karttulan kartta-alueiden kallioperä. Summary: Pre-Quaternary rocks of the Rautalampi and Karttula map-sheet areas. Suomen geologinen kartta 1:100 000, kallioperäkarttojen selitvkset, lehdet 3223 ja 3224. Geologian tutkimuskeskus. 81 p. Available at: https://tupa.gtk.fi/kartta/kallioperakartta100/kps_3223_3224.pdf

Salvador, D. 2021. Beneficiation of Raisjoki, Emas and Koivuniemi graphite occurrences-Finland. Geological Survey of Finland, Open File Research report C/MT/2021/1. Unpublished report.

Stipp, M., Stunitz, H., Heilbronner, R. & Schmid, S. 2002. The eastern Tonale fault zone: a ´natural laboratory´ for crystal plastic deformation of quartz over a temperature range from 250 to 700 ºC. Journal of Structural Geology 24, 1861–1884.

APPENDICES

Appendix 1. Laboratory analysis information.

Eurofinns labtium analysis information

Analysis report nr.	Order nr.
31449	40275
38976	40295

Appendix 2. Drillholes and drillhole profiles.

HOLE_ID	X-TM35FIN	Y-TM35FIN	Z-N2005N00	Length	azimuth	Dip
N4442017R16	6952473.415	490245.776	101.63	146.2	45	45.3
N4442017R17	6952448.231	490220.887	101.665	101	45	44.3
N4442017R18	6952559.504	490190.253	101.433	103.7	45	45
N4442017R19	6952523.757	490154.775	101.85	47.7	45	45
N4442017R20	6952437.651	490352.593	101.618	39	45	45
N4442017R21	6952395.334	490309.034	101.876	109.45	45	45.6
N4442017R22	6952429.951	490202.944	102.092	89.5	45	44.6
N4442017R23	6952498.068	490338.516	101.2	46.2	45	45
N4442017R24	6952589.993	490480.03	99.835	80.45	360	45.4
N4442018R33	6951600.169	490822.113	102.343	98.9	50	45
N4442018R34	6951550.535	490861.312	102.167	113.4	50	46.7
N4442018R35	6951486.361	490903.798	101.17	143.2	50	45
N4442018R36	6951512.168	490972.019	102.029	144.5	50	45

Appendix 2. Cont.

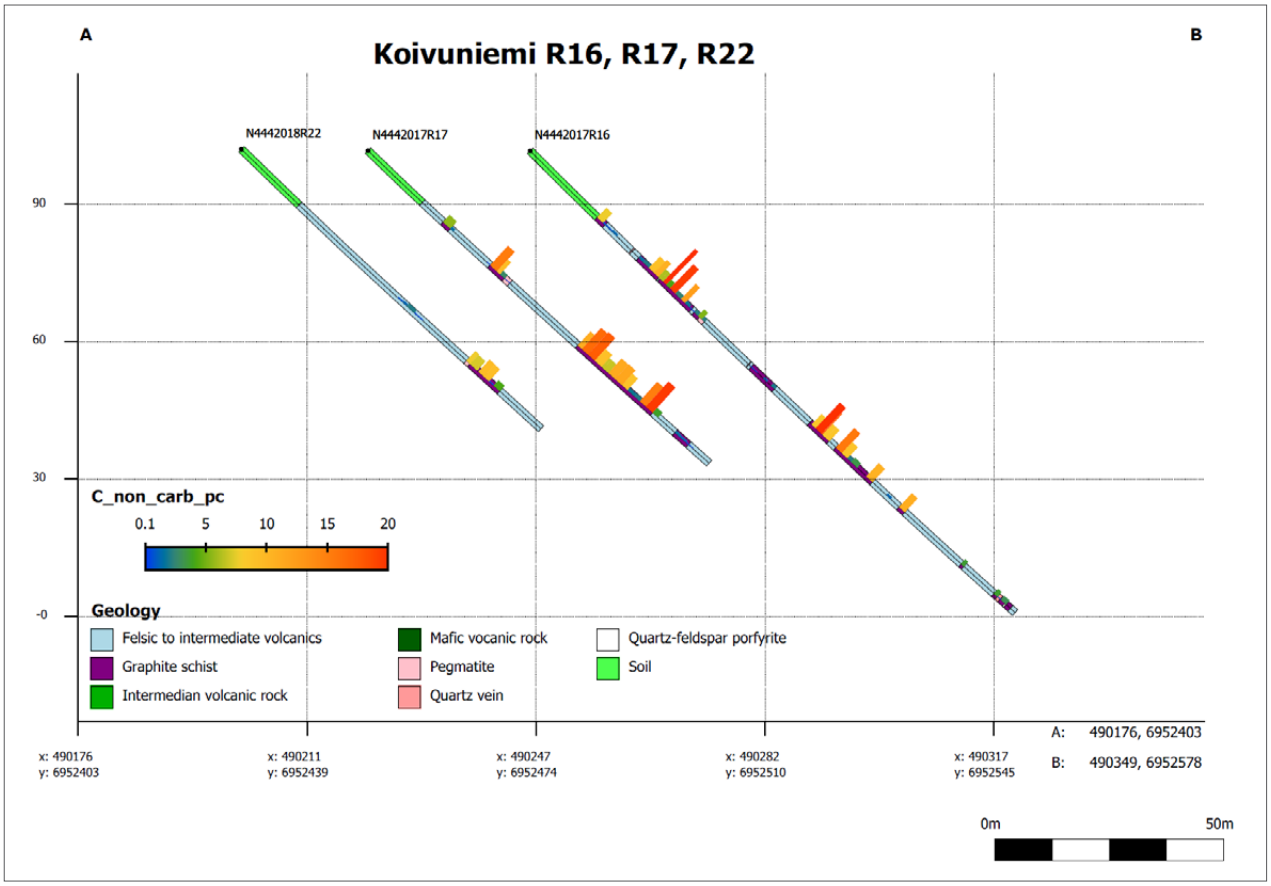

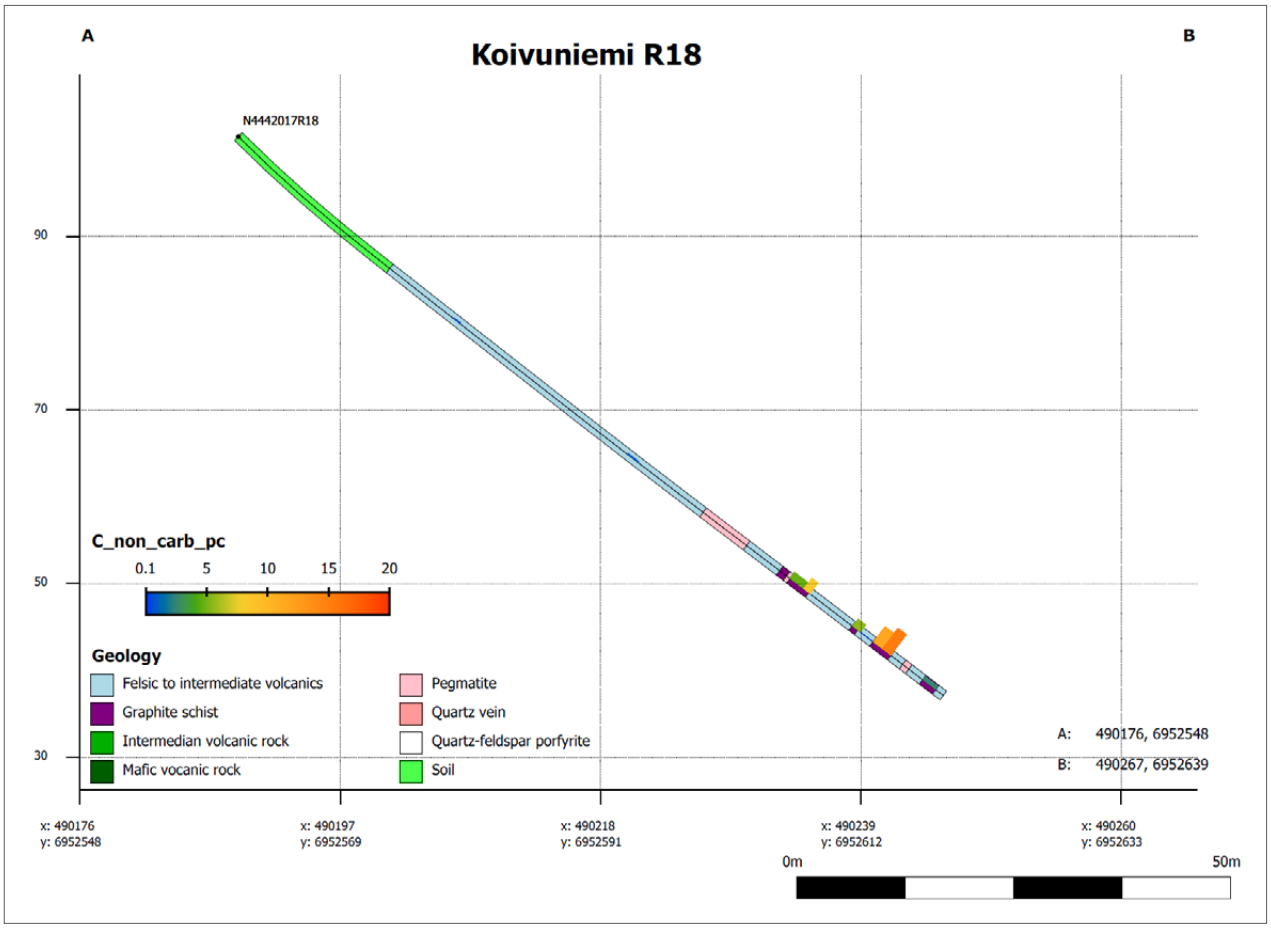

Appendix 2. Cont.

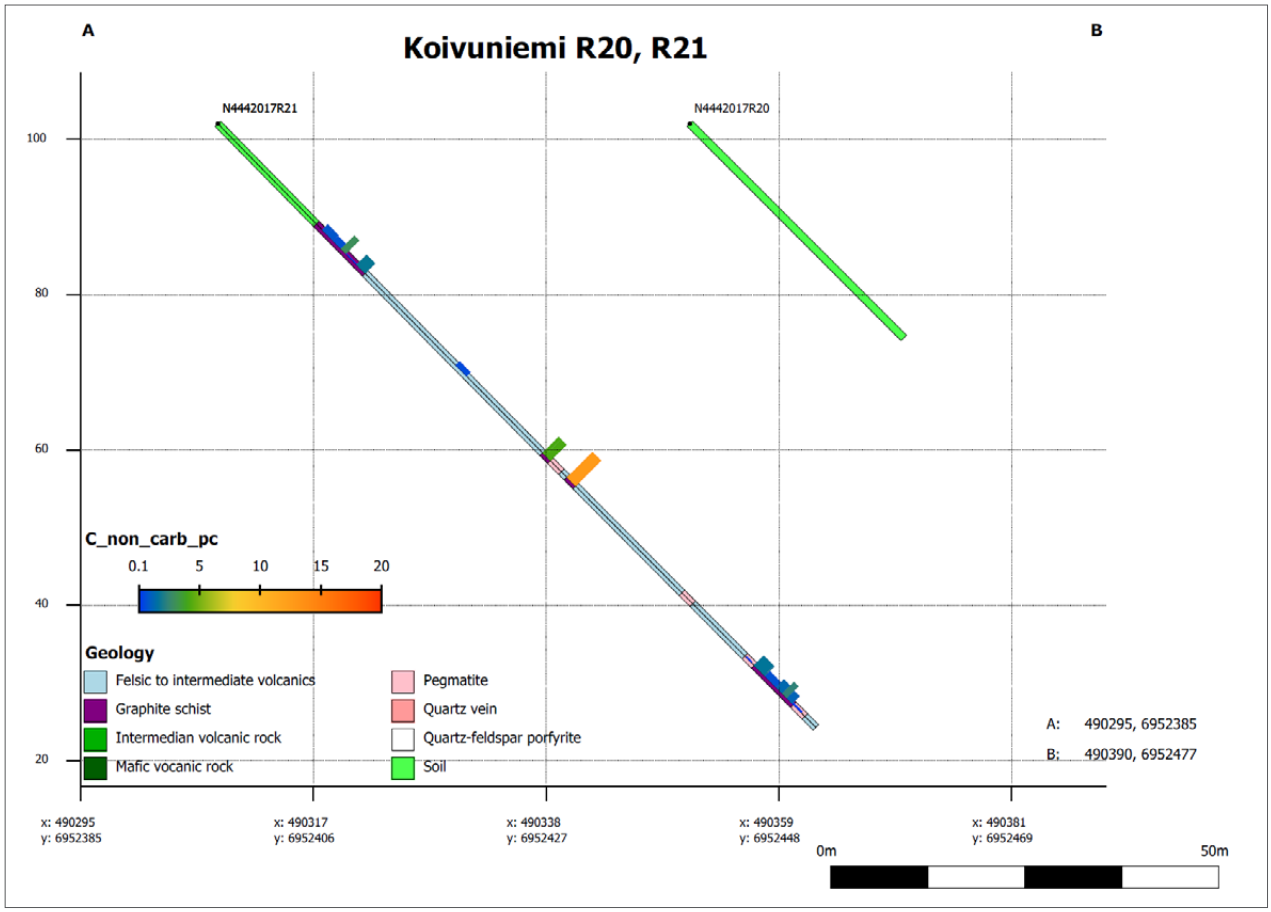

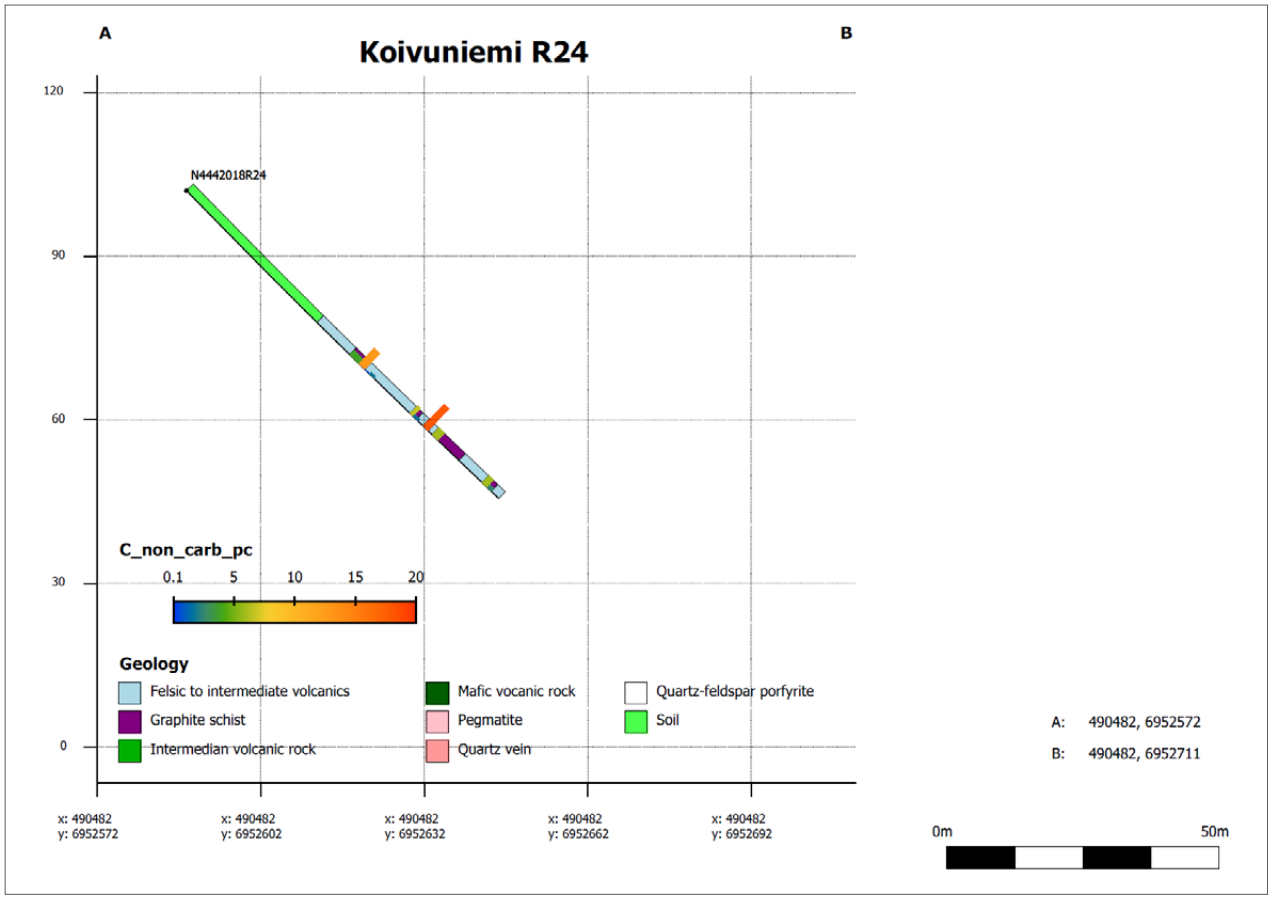

Appendix 2. Cont.

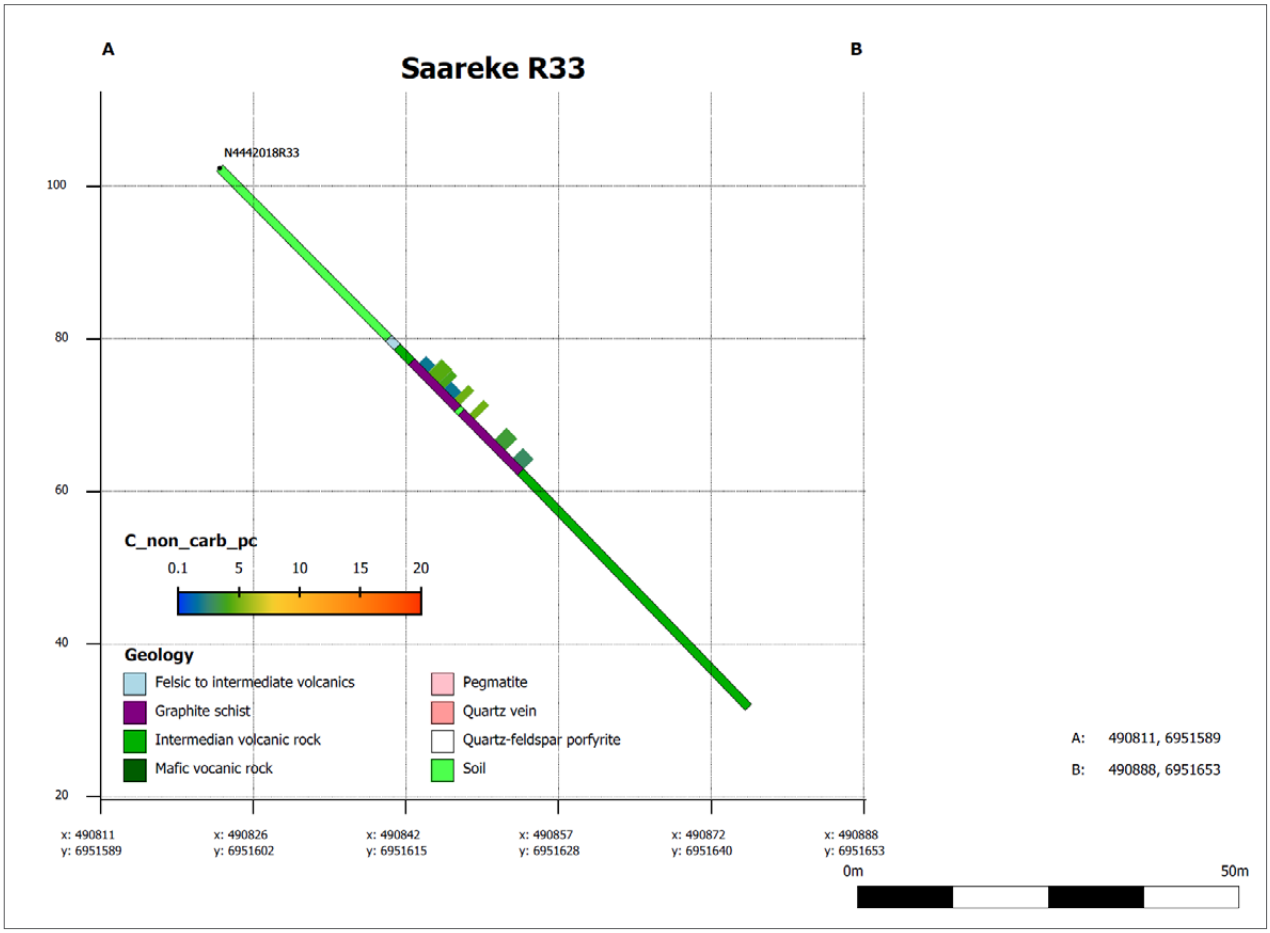

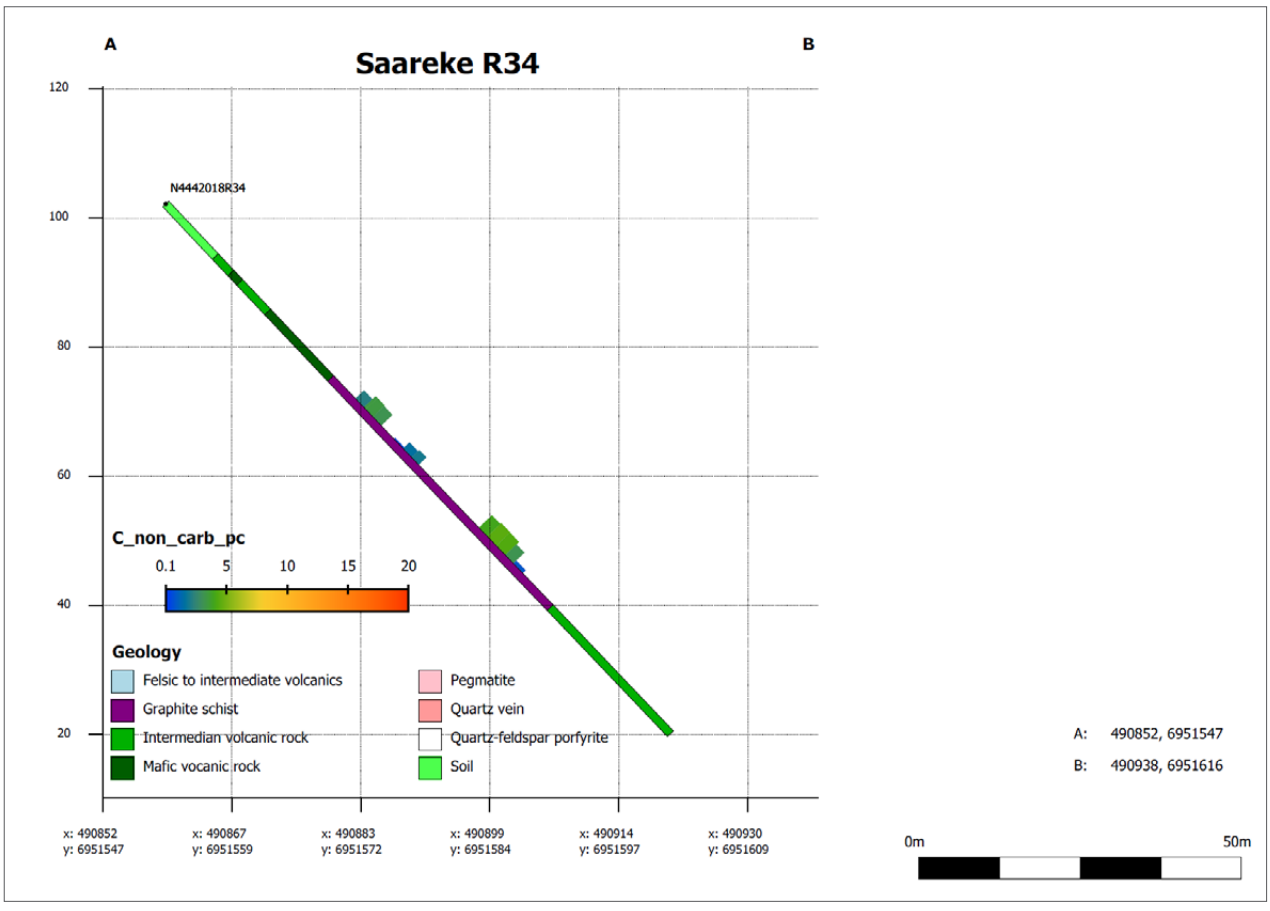

Appendix 2. Cont.

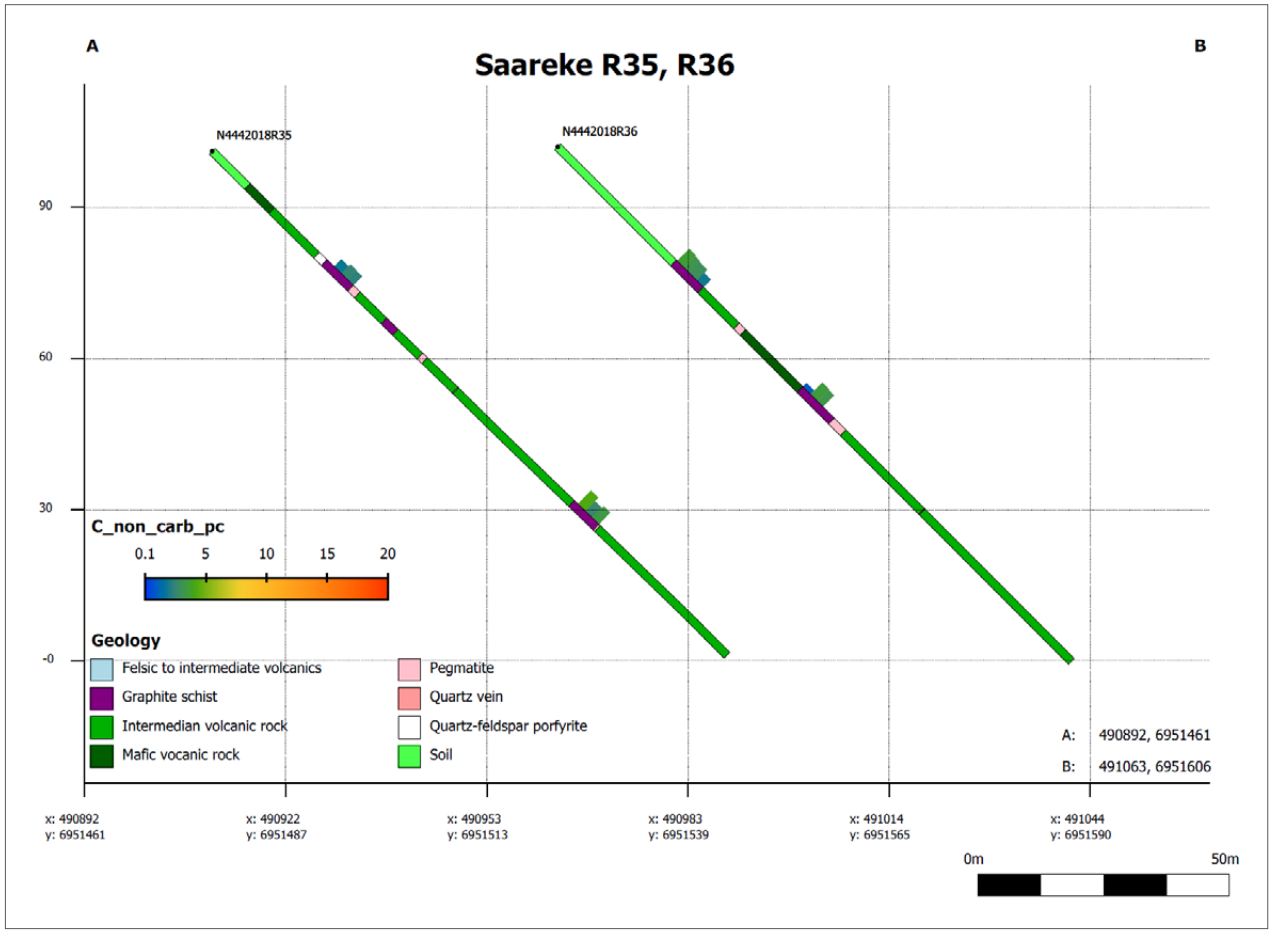

Appendix 3. SEM-EDS – analysis data. Numbering after sample-id indicate spot analysis number.

Specimen	N4442017R16 40.80						N4442017R18 32.30					N4442018R24 44.75				N4442018R34 54.55			
Analyse number	1	2	3	4	5	6	1	2	3	4	5	1	2	3	4	1	2	3	4
C (wt %)	98.86	98.78	98.92	98.64	98.9	98.06	97.58	97.76	97.7	97.69	97.74	98.84	98.3	98.73	98.05	97.15	97.7	97.32	97.09
Na							0.1	0.11	0.11	0.09	0.12	0.07	0.12	0.17	0.16			0.14	
Mg							0.14	0.11	0.12	0.11	0.1	0.06	0.05			0.12	0.1		0.15
Al							0.47	0.46	0.47	0.47	0.46	0.28	0.47	0.36	0.57	0.35	0.38	0.5	0.53
Si	1.14	1.22	1.08	1.36	1.1	1.94	0.88	0.9	0.92	0.93	0.95	0.55	0.79	0.74	1.12	1.32	1.25	1.31	1.26
Fe							0.6	0.47	0.47	0.45	0.42	0.2	0.27			0.59	0.57	0.61	0.77
K							0.22	0.19	0.21	0.25	0.21				0.1			0.12	
F																0.31			
Ca																0.31			0.2

Appendix 4. Detailed list of petrographical observations and carbon contents of whole rock-analysis.

Locality	Analyse number	Sample number	Thin section number	Graphite (%)	Quartz (%)	Plagioclase (%)	K-feldspar (%)	Biotite (%)	Muscovite (%)	Other mineral (%)	Pyrite (%)	Pyrrhotite (%)	Accessory/ trace minerals	Alteration 1	Alteration intensity	Alteration 2	Alteration 2 intensity	Alteration 3	Alteration 3 intensity	811L (wt %)	816L (wt %)	816L (wt %)
Koivuniemi	N4442017R16 40.70-41.70	N4442017R16 40.80	180527	25	40	10		15			10									28.1	1.49	26.6
Koivuniemi	N4442017R16 68.40-69.40	N4442017R16 69.20	180528	<1	40	15		20		Sillimanite (15)	4		Rutile	Sericite	1					0.3	<0.05	0.26
Koivuniemi	N4442017R16 89.00-91.00	N4442017R16 90.90	180529	10	30	30		10	<1		15		Rutile	Sericite	3					8.45	<0.05	8.59
Koivuniemi	N4442017R17 36.55-38.55	N4442017R17 36.65	180530	20	35	20		10	<1		10		Rutile	Sericite	2	Saussurite	2			15.5	0.19	15.3
Koivuniemi	N4442017R17 75.50-77.10	N4442017R17 76.70	180531	10	40	10		15	1			25								8.65	<0.05	8.92
Koivuniemi		N4442017R18 32.30	180532	3	30	15	20	30	1		2		Garnet	Sericite	1							
Koivuniemi	N4442017R18 94.80-96.10	N4442017R18 95.15	180533	25	30	25		10			10		Chalcopyrite	Sericite	3					15.8	0.53	15.3
Koivuniemi	N4442017R21 19.15-21.15	N4442017R21 20.80	180534	1	30	20	10	30		Garnet (3)	4		Zircon, Apatite	Sericite	1					0.82	<0.05	0.79
Koivuniemi	N4442017R21 43.65-45.65	N4442017R21 44.25	180535	1	25	25	15	20			9		Zircon, Chalcopyrite	Sericite	2	Saussurite	2			0.55	<0.05	0.51
Koivuniemi	N4442017R21 64.00-65.60	N4442017R21 64.75	180536	15	40	15		20			10			Sericite	1					12.8	0.1	12.7
Koivuniemi	N4442018R22 71.00-72.60	N4442018R22 71.50	180537	15	25	20		15	10		15									9.55	<0.05	9.54
Koivuniemi	N4442018R24 44.75-46.30	N4442018R24 44.75	180538	20	20	35		15			10		Zircon	Saussurite	2					12.8	<0.05	12.9
Saareke	N4442018R33 38.20-40.20	N4442018R33 39.40	180596	7	30	30		10	<1	Hornblende (10)	12		Chalcopyrite, Sphalerite	Sericite	1	Chlorite	2			4.47	0.07	4.4
Saareke	N4442018R34 52.80-54.70	N4442018R34 54.55	180597	5	30	25		10		Augite (10), Chlorite (5)	15		Chalcopyrite, Sphalerite	Sericite	2	Saussurite	2	Chlorite	1	1.69	0.12	1.58
Saareke	N4442018R34 69.80-71.70	N4442018R34 70.30	180598	6	30	25		5		Calcite/ dolomite (5)	22		Chalcopyrite, Sphalerite	Sericite	2					4.47	0.49	3.98
Saareke	N4442018R35 37.00-38.70	N4442018R35 37.60	180599	5	25	25		15		Hornblende (10)	15		Chalcopyrite, Sphalerite	Sericite	2	Chlorite	1			2.54	0.21	2.33

Mineral modal amounts as % are visible estimations with microscope
Alteration intensity: 1- weak, 2 - moderate, 3 - strong

All GTK's publications online at hakku.gtk.fi